Materials Advances

ROYAL SOCIETY OF CHEMISTRY

REVIEW

View Article Online
View Journal | View Issue

Cite this: *Mater. Adv.*, 2022, 3, 3070

Bioinspired carbon nanotube-based materials

Yi Fan,†[a] Yaqi Hou,†[ab] Miao Wang,*[c] Jing Zheng*[a] and Xu Hou*[abd]

Bioinspired materials exhibit unique design strategies derived from nature, with remarkable biomimetic structures and identical biological features. Among them, bioinspired carbon nanotube (CNT)-based materials have attracted great interest because CNTs, as construction materials, have several advantages in terms of their structural, chemical, and physical properties. In this review, we present a systematic overview of the progress of CNT-based materials with design inspiration from nature in recent years. Firstly, the advantages of CNTs in the fabrication of bioinspired CNT-based materials are summarized, including their unique structure with high mechanical properties, controllable functionalized surfaces, and high conductivity. Secondly, different design strategies are categorized, where CNTs can directly act as artificial nanochannels, arrange to form CNT-assembled structures, or combine with inorganic, organic, and polymer materials to achieve CNT composites. Thirdly, their applications in reinforcement materials, energy conversion, nanopatterned surfaces, dry adhesion, and bioengineering are discussed. Finally, further challenges and perspectives are outlined, which will offer a comprehensive view and inspiration for scientists to develop bioinspired CNT-based materials with more advanced and beneficial performances.

Received 25th January 2022,
Accepted 18th February 2022

DOI: 10.1039/d2ma00086e

rsc.li/materials-advances

1. Introduction

Over billions of years, biological systems have evolved into sophisticated structures with elaborate functions. Thus, ideas from the study of living organisms to create novel materials with outstanding characters (*e.g.*, simplified devices, multi-function, superior performances, and intelligence activity) have proven to be important for solving problems in challenging situations. Bioinspired materials, products of this learning process by mankind, have been considerably utilized in aerospace, environmental treatment, energy conversion/storage, and biotechnology.[1–8] Bioinspired materials are usually made

[a] *State Key Laboratory of Physical Chemistry of Solid Surfaces, College of Chemistry and Chemical Engineering, Xiamen University, Xiamen 361005, China. E-mail: houx@xmu.edu.cn, zjing@xmu.edu.cn*
[b] *Research Institute for Biomimetics and Soft Matter, Fujian Provincial Key Laboratory for Soft Functional Materials Research, Jiujiang Research Institute, College of Physical Science and Technology, Xiamen University, Xiamen 361005, China*
[c] *College of Materials, Xiamen University, Xiamen 361005, China. E-mail: miaowang@xmu.edu.cn*
[d] *Innovation Laboratory for Sciences and Technologies of Energy Materials of Fujian Province (IKKEM), Xiamen 361102, China*
† These authors contributed equally to this work.

Yi Fan

Dr Yi Fan received her PhD Degree in 2021 under the supervision of Prof. Xu Hou at Xiamen University. She currently works as a Postdoctoral Fellow with Prof. Xu Hou at Xiamen University. Her current scientific interests are focused on bioinspired smart materials, liquid gating technology, and visible chemical detection.

Yaqi Hou

Dr Yaqi Hou received her PhD Degree in 2018 under the supervision of Prof. Chen Zhang and Jianguo Mi at Beijing University of Chemical Technology. Currently, she works as a Postdoctoral Fellow with Prof. Xu Hou at Xiamen University. Her current scientific interests include interfacial science, bioinspired nanofluidic ionics, and nanomaterials for ionic/molecular detection, seawater desalination and energy generation applications.

of single or multi-component synthetic materials (as the construction materials). To date, numerous synthetic materials have been manufactured into bulk with particular structures, properties, and functions to construct bioinspired materials. The examples of recently developed bioinspired materials are commonly derived from the two bioinspired design strategies, *i.e.*, mimicking structures of natural materials (*e.g.*, chemical syntheses and biomimetic polymers toward bio-based materials, self-assembled bioinspired nanocomposites materials, and emerging artificial wood materials) and mimicking functions of living matters (*e.g.*, gas-involved (photo) electrocatalysis with the regulation of biomimetic wetting in energy conversion, bioinspired nanofluidic iontronics, non-fouling surfaces with bioinspired dopamine chemistry and zwitterionic polymers).[9–15]

To choose the appropriate materials to construct bioinspired materials, it is usually necessary to evaluate their application value in bioinspired design strategies. However, few materials have similar features to carbon nanotubes (CNTs), which are composed of nanoscale structures and possess outstanding chemical and physical properties.[3,16–18] CNTs, discovered in 1991 by Iijima, are regarded as graphene sheets rolled up along Bravais lattice vectors to form hollow cylindrical nanostructures.[19] There are mainly two types of CNTs, *i.e.*, single-walled carbon nanotubes (SWCNTs, composed of one single graphene layer) and multi-walled carbon nanotubes (MWCNTs, formed from multiple graphene layers). The diameters of SWCNTs are generally narrower than that of MWCNTs, where the diameter of SWCNTs is in the range 0.8–2 nm and that of MWCNTs in the range 5–20 nm.[17,20] Different formations of SWCNTs by rolling of the graphene sheets along lattice vectors can result in three types of tubes (armchair, zigzag, and chiral tubes).[20] The hollow morphology with nanoscale diameters and atomically smooth inner surfaces of CNTs make them ideal artificial materials with nanochannel geometries. Also, with the strongest carbon bonds, CNTs possess chemical stability, large surface with strong adsorption, low weight, and high mechanical strength. Together with the physical properties of electrical conductivity and possibility of versatile modifications to obtain special performances, CNTs are expected to be the most valuable materials in electronics, nanotechnology, materials science, and bioengineering.[5,20–34] Nowadays, CNTs are easily obtained at a very low price due to the development of synthetic techniques. However, the demands from worldwide commercial interest will be satisfied by fabricating bioinspired CNT-based materials combined with the superior properties of CNTs, such as extremely high mechanical strength, electrical conductivity and multifunction.[17] Fig. 1 shows the timeline of the major advances of carbon nanotubes in their 30 year history.

Here, we define ''bioinspired CNT-based materials'' as materials that are inspired by biological structures or functions and developed based on single CNT, assembled CNT or CNT composites for reinforcement, energy conversion, dry adhesion, and bioengineering applications. A systematic review on the recent progress of bioinspired CNT-based materials is

Miao Wang

Dr Miao Wang received her B.S. Degree (2010) from Nanjing University of Science and Technology (NJUST). She obtained her PhD Degree (2016) from NJUST under the guidance of Prof. Qiang Li. She did postdoctoral research in Prof. Xu Hou's group at Xiamen University (2016–2020). She is currently an Assistant Professor at Xiamen University. Her research interest is focused on carbon nanotube-based smart materials and devices with their applications in heat transfer, thermal management, nanofluidics, energy harvesting and seawater desalination.

Jing Zheng

Dr Jing Zheng received his BS Degree in Chemistry from the University of Science and Technology of China in 2012. Then, he began his PhD study at the University of Hong Kong under the supervision of Prof. Jinyao Tang. After receiving his PhD Degree, he worked as a Post-Doctoral Researcher at the University of Hong Kong in 2018–2021. In 2022, he officially joined Xiamen University as a Full Associate Professor.

Xu Hou

Prof. Xu Hou received his B.S. Degree (2006) from Sichuan University. He completed his PhD Degree (2011) at the National Center for Nanoscience and Technology under the direction of Prof. Lei Jiang. He did postdoctoral research in Prof. Joanna Aizenberg's group at Harvard University (2012–2015). He joined Xiamen University as a Full Professor in 2016 and his current scientific interest includes liquid gating technology, membrane science and technology, interfacial science, and micro/nano fabrication for energy, environmental and biomedical applications.

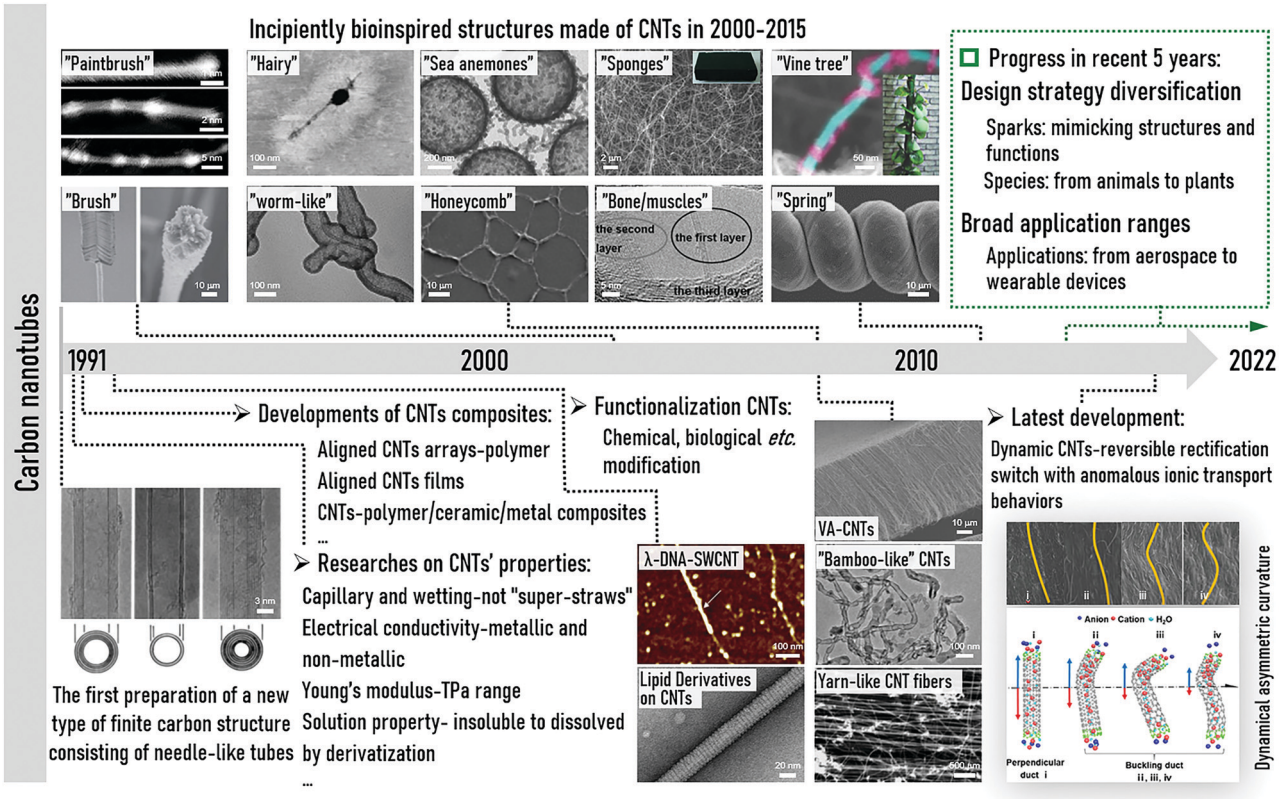

Fig. 1 Timeline of the major advances of CNTs in their 30-year history. CNTs were firstly prepared in 1991. Reproduced with permission.[19] Copyright 1991, Nature. Various studies have been conducted on their properties (*e.g.*, capillary and wetting,[35] electrical conductivity,[36] Young's modulus,[37] and solution properties[38]). In the same period, CNT composites have been developed (*e.g.*, aligned CNT array-polymer,[39] aligned CNT films,[40] and CNT-polymer/ceramic/metal composites[41]). Also, there have been many functionalizations, normally chemical or biological modifications and CNT studies (*e.g.*, λ-DNA-SWCNT. Reproduced with permission.[42] Copyright 2003, the American Chemical Society. Lipid derivatives on CNTs. Reproduced with permission.[43] Copyright 2003, Science.). Bioinspired CNT-based materials emerged in the early 20th century, normally having similar structures to natural organisms. In 2000–2015, various bioinspired structures were made by CNTs with morphologies of "brush" (Reproduced with permission.[44] Copyright 2005, Nature.), "paintbrush" (Reproduced with permission.[45] Copyright 2006, the American Chemical Society.), "worm-like" (Reproduced with permission.[46] Copyright 2006, Wiley-VCH.), "hairy" (Reproduced with permission.[47] Copyright 2007, Wiley-VCH.), "honeycomb" (Reproduced with permission.[48] Copyright 2009, Wiley-VCH.), "sea anemones" (Reproduced with permission.[49] Copyright 2008, Wiley-VCH.), "sponges" (Reproduced with permission.[50] Copyright 2009, Wiley-VCH.), "spring" (Reproduced with permission.[51] Copyright 2012, Wiley-VCH.), "vine tree" (Reproduced with permission.[52] Copyright 2014, Wiley-VCH.), *etc.*, and even adopted the "bone/muscle" strategy (Reproduced with permission.[53] Copyright 2009, Wiley-VCH.), *etc.* New structures of CNTs, such as VA-CNTs (Reproduced with permission.[54] Copyright 2004, Science.), "bamboo-like" CNTs (Reproduced with permission.[55] Copyright 2005, Wiley-VCH.), and CNT yarn (Reproduced with permission.[56] Copyright 2010, Wiley-VCH.), have also laid the foundation for the design of novel bioinspired CNT-based materials. In the upper right corner, the progress of bioinspired CNT-based materials in the recent 5 years is summarized. Besides, our group also has paid great attention to CNTs, including bioinspired nanoscale channels,[57–60] CNT-based desalination,[61–65] and CNT-based nanogenerators.[66] One study is shown in the bottom right corner: dynamic CNTs. Reproduced with permission.[65] Copyright 2019, Wiley-VCH.

provided, including superior properties of CNTs in construction, their design strategies, and applications (Fig. 2). The following content is mainly composed of three parts, as follows: (i) the superiorities of CNTs in designing bioinspired CNT-based materials; (ii) the design strategies for bioinspired CNT-based materials: CNTs directly as artificial nanochannels or as construction materials with CNT-assembled structures and CNT composites; and (iii) typical examples of bioinspired CNT-based materials in applications of reinforcement materials, energy conversion, nanopatterned surfaces, dry adhesion, and bioengineering. Finally, the current challenges and future prospects in the development of CNTs are briefly summarized. We envision that this work will inspire researchers to focus on the extensive application of bioinspired CNT-based materials and eventually realize the application of CNTs in practice.

2. Superiorities of CNTs in designing bioinspired CNT-based materials

2.1 Unique structure

Owing to the intrinsic morphology of hollow cylinders with nanometer diameters and allotropes of carbon made of only carbon atoms with chemical inertness through sp^2 bond networks, CNTs possess a unique structure and properties. Hollow nanoscale channels have the equivalent size to that of

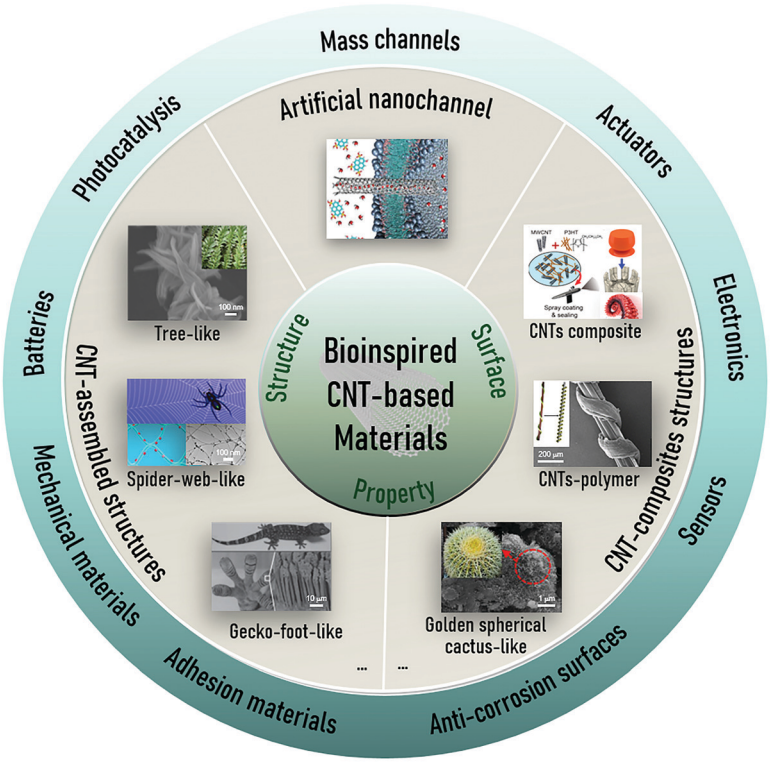

Fig. 2 Based on the superiorities of CNTs in terms of structure, surface, and properties, diverse design strategies are used to fabricate bioinspired CNT-based materials in various fields. Artificial mass transport. Reproduced with permission.[67] Copyright 2017, Science. CNT-based tree-like materials in photocatalysis. Reproduced with permission.[68] Copyright 2015, Elsevier. CNT-based spider-web-like materials in designing mechanical materials. Reproduced with permission.[69] Copyright 2016, the American Chemical Society. CNT-based gecko-foot-like materials in designing adhesion materials. Reproduced with permission.[70,71] Copyright 2012, Wiley-VCH. Copyright 2008, Science. CNT-based golden spherical cactus-like materials in designing anti-corrosion surfaces. Reproduced with permission.[72] Copyright 2018, Elsevier. CNT-polymer materials in electronics. Reproduced with permission.[73] Copyright 2019, the American Chemical Society. CNT composites in actuators. Reproduced with permission.[74] Copyright 2021, the American Chemical Society.

endogenous protein channels, making CNTs ideal materials for studying the transport of ions and molecules. Resulting from their covalent sp^2 bonds, CNTs are the strongest and stiffest materials reported to date with a tensile strength of up to 100 GPa and Young's modulus of 1 TPa (about 5-times higher than that of steel with a value of 210 GPa). The highest mechanical property of CNTs make them distinguished reinforcement materials in designing bioinspired CNT-based materials, mostly working as frames or substrates.[16,75–78] Piling or stacking individual CNTs also results in the formation of patterned architectures in bioinspired CNT-based materials with interesting behaviors (*e.g.*, high strength and toughness, and high dry adhesion).[79] More importantly, the elaboration of other characteristics in bioinspired CNT-based materials is related to the natural structure of CNTs.

2.2 Controllable surface

CNTs have nanoscale tubular structures with a surface area of up to 50–200 $m^2\ g^{-1}$.[80] Due to the presence of the strongest non-polar C–C bonds and hydrophobicity of pure sp^2 hybrid carbon bonds, CNTs are naturally hydrophobic and insoluble in aqueous and organic solvents. Studies have indicated that bioinspired CNT-based materials can be obtained with rough surfaces and low surface energy by introducing CNT fragments.[18,81–83] However, the hydrophobicity of CNTs restricts the applicability of bioinspired CNT-based materials. In bioengineering, the excellent along the tubular axis, which is different from graphene and the biocompatibility of bioinspired CNT-based materials with biosafety is necessary.[24,84,85] Modification of the hydrophilic groups (*e.g.*, carboxylic, carbonyl, and hydroxyl through well-established methods) on the surface of CNTs will overcome the existing bottlenecks. Due to the natural mechanical behavior and functionalized surfaces of CNTs, the bioinspired CNT-based materials will perform admirably in bioskeletons and biosubstrates. To date, several chemical modifications (*e.g.*, minimum alteration by non-covalent functionalization and permanent modification by covalent functionalization) and doping methods have been developed for the functionalization of CNTs.[86] These approaches allow the surfaces of CNTs to become controllable functionalized surfaces by integrating various functional groups, and also allow additional behaviors to be obtained through the functionalization process. The controllable functionalized surface can improve the properties of CNTs, which is another superiority to enhance the performances of bioinspired CNT-based materials.[87–93]

2.3 High conductivity

As carbon materials, CNTs are either metallic or semiconducting along their tubular axis, which is different from graphene and other carbon materials. Thus, by changing the alignment, diameter, aspect ratio, and chirality in CNTs, the electronic conductivity of bioinspired CNT-based materials can be regulated.[18] Befitting from the prominent high conductivity, artificial mass transport nanochannels, and good mechanical properties of CNTs, bioinspired CNT-based materials have become popular alternative materials to solve the problems in energy conversion, for example, improving the poor electrical conductivity, quick capacity decay, and lithium anode erosion in lithium–sulfur (Li–S) batteries, solving the problems of high volume expansion or contraction in the processes of charging and discharging, poor cyclability and rate capability of oxides in lithium-ion batteries (LIBs), abating capacity fading and increasing inferior rate in sodium-ion batteries (SIBs), and even promoting photoenergy conversion in photocatalysis. Moreover, the high conductivity of bioinspired CNT-based materials make them valuable for application in biosensors and bioelectronics. In the system, once specific molecules or physical stimuli are recognized by the decorated functional groups on the surface of CNTs through specific interactions, the CNTs in the bioinspired materials can output the correlated information with electrical signals. Apparently, smart bioinspired CNT-based materials can obtain exceptional electrical responses due to the integration of CNTs.

Table 1 lists the popular mimicked living organisms based on CNTs in the last 5 years, as well as the chemical components of bioinspired CNT-based materials, the functional activities of CNTs in bioinspired materials, and their potential applications. In the next section, the corresponding design strategies for bioinspired CNT-based materials are further reviewed.

3. Design strategies

Among the synthetic materials adopted for the fabrication of bioinspired materials, CNTs are regarded as unique materials. Their high availability in the formation of bioinspired

Table 1 Popular mimicked living organisms for bioinspired CNT-based materials in biostructure design

Inspiration	Material & hierarchical structure	Functional activities	Potential applications	Ref.
Silk fiber	CNT-SF & G–G fibers	High mechanical framework for fibers	Structural materials	94
Spider silk	BISS-SWCNTs fibrils	Stable structural substrate and conductive	Electro-mechanical materials	69
Muscle	CNT yarn (by mechanical training)	frameworks for electron transfer		95
Mussel	Mussel-inspired chemistry: CNTs/PDA GW-hydrogel	Nanoreinforcements for increasing the conductive and mechanical properties	Self-adhesive bioelectronics	96
	TA-CNTs			97
	CNTs/PDA/PANi	One-, and two-dimensional conductivity materials	Flexible thermoelectric generators	98
Nacre	CNT@PANI/rGO/TA	Reinforcement for high strength and conductivity	Portable and wearable electrical devices	99
Salvinia molesta leaf	E-glass/MWCNTs (by ISA-3D)	Mechanical support and surface roughness donor	3D printed materials	83
Wood	PTCDA/NC/CNT composite	3D conductive frameworks with micro/nanotunnels structures for ionic/electronic transport	Batteries	100
Spider web	MWCNT/γ-Fe_2O_3 web	Mechanical support	High-performance energy storage materials	101
Nacre	CNTs/PVP	Conductive network	Batteries	102
Stem	Sn_4P_3@CNT/C composite	Electron expressway and mechanical support	Batteries	103
Ear-of-wheat	MWCNTs/MONPs composite	Conducting network	Batteries	104
Trees	ciO_2/CNT composites	Direct electron transport channels in photocatalysis with large specific surface and thermoelectric conductivity	Photocatalysis materials	68
Golden spherical cactus	PSU/CNTs/FEP with microsphere and nanothorns	GC-like structure donor and the network structures that conduct electrons	Superhydrophobic materials	72
Gecko feet	VA-CNT strands	Adhesion strength	Adhesion materials	105
	CNTF	Adhesion to electrical and thermal management		93
	3DP GC	Enhancement in flexural strength	Energy conversion, energy storage, environmental or electronic systems	106
Chameleon	HPC-PACA-CNT composite	Enhancement in conductivity and capability of reporting stimuli through resistance	Multifunctional flexible E-skins	107
Homarus americanus claws	Radial and circumferential aligned MWCNT-S	Multifunctional nanofillers with unique structures and excellent mechanical properties	Aerospace, mechanical, and tissue engineering	108
Evaporation of sweat Transpiration of plants	Porous-structured CNT films	Optical absorptivity from π-band optical transitions with a wide range of 200 nm–200 μm and fast water transport channels	Solar hygiene systems, freshwater distillation, and electrical power generation	109
Polar bear pelt	Porous Ag/cellulose/ CNT-laminated nanofiber membrane	High solar radiation absorptivity	Thermal control materials, smart garments, and wearable electronics	110
Moth eye	SWCNT coating-deposited Si	Optical properties with refraction index n_{eff} = 1.01–1.10	Anti-reflective coatings	111

CNT-based materials mainly comes from their superior chemical and physical properties with unique hollow structure, high strength, high toughness, electrical conductivity, chemical stability, *etc.*, and their diverse construction assemblies and design strategies.[67,83,98–100] In this section, we first discuss the individual CNTs with 1D natural nanochannels to mimic protein channels, and then a series of bioinspired CNT-based materials with the design strategies of CNT-assembled structures (*e.g.*, metal oxide-anchored CNTs, CNT fibers, CNT yarns, CNT bundles, CNT web, and CNT array) and the CNT composites structures (*e.g.*, CNT-polymer composite, CNT layer-by-layer composite, and CNT hydrogel).

3.1 Directly as artificial nanochannels

Biological nanochannels, such as water, calcium (Ca^{2+}), and sodium (Na^{+}) protein channels, play critical roles in physiological processes, sophisticatedly regulating the release of ions and biomolecules.[112,113] Inspired by these subtle nanostructures, creating artificial materials with similar morphologies by replicating biological processes has become a popular way to understand cellular events. CNTs, a promising allotrope of carbon, are composed of only carbon atoms. Their seamless cylindrical morphology with nanoscale inner diameter (for SWCNTs, their diameters are 1–6 nm, while that for MWCNTs is 2–100 nm) makes them ideal artificial nanochannel platforms for mimicking the mass transport in nano-confined space. When molecules such as water molecules pass through these nanochannels, the inner graphitic walls and confined smooth nanochannel structures of CNTs enhance the transport of water.[114]

Computational chemistry has become a very popular and instructive method to evaluate the mass transport in CNT-based nanochannel materials. As shown in Fig. 3a, one study utilized molecular dynamics (MD) simulations to explore the ion permeation and selectivity in series computer-designed CNT-based biomimetic nanopores, in which the series models (C0, C-2, C-4 and C-1, where the C0 model nanopore has two carboxylate and two amine groups (net charge 0), C-2 model nanopore has two carboxylate groups (net charge −2), C-4 has four carboxylate groups (net charge −4), and C-1 has two

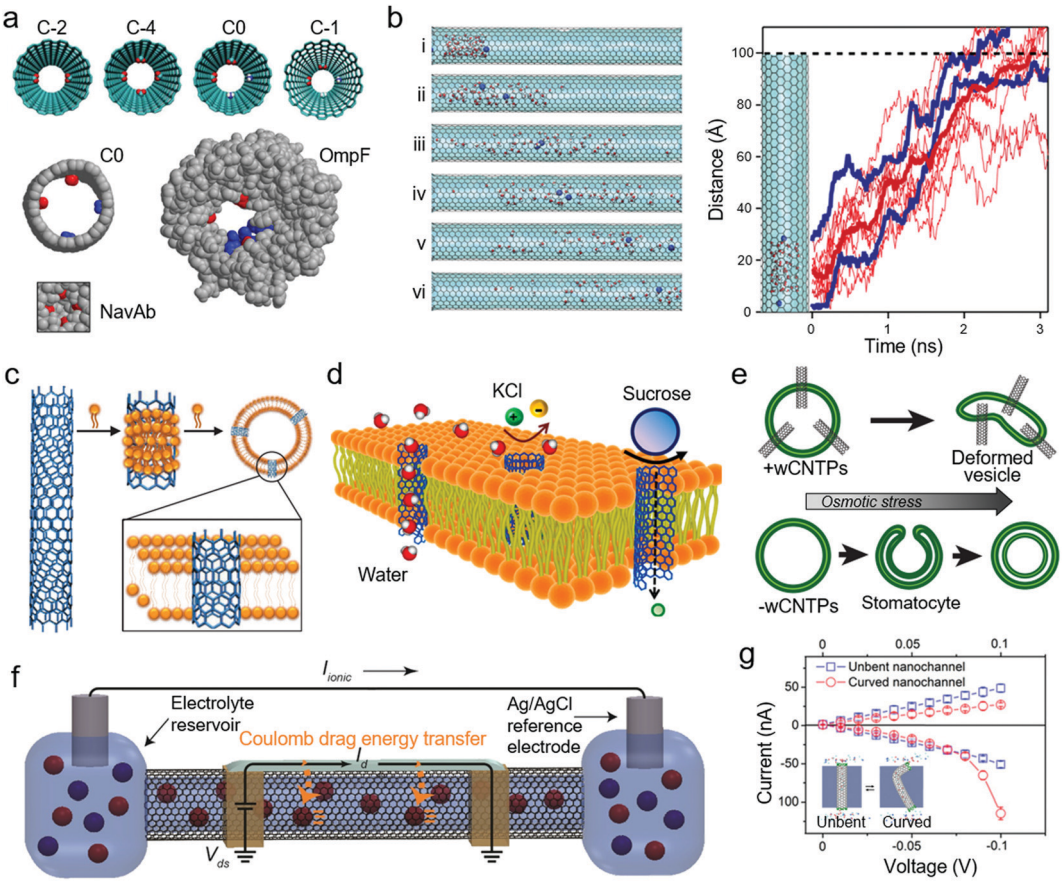

Fig. 3 (a) Simulation of derivatized CNTs and comparison of the C0 model nanopore with two biological nanopores. Reproduced with permission.[115] Copyright 2012, National Academy of Sciences. (b) MD simulations of water and ion transport in CNTPs. Reproduced with permission.[116] Copyright 2019, the American Chemical Society. (c) Preparation and incorporation of CNTPs in liposomes. Reproduced with permission.[117] Copyright 2014, Nature. (d) Osmotically driven transport in CNTPs. Reproduced with permission.[118] Copyright 2014, the American Chemical Society. (e) Presence of CNTPs resulted in distinct polymersome responses to osmotic stress. Reproduced with permission.[120] Copyright 2018, Wiley-VCH. (f) Electrically actuated, CNT-based biomimetic ion pump. Reproduced with permission.[121] Copyright 2019, the American Chemical Society. (g) Dynamic curvature nanochannel-based membrane. Reproduced with permission.[125] Copyright 2019, Wiley-VCH.

carboxylate and one amine group (net charge −1)) of filters were distributed, deriving the natural Ca^{2+} and Na^{+} channels.[115] These resultant nanopores had comparable ion selectivity with the structures of pivotal proteins in bacterial porins and voltage-gated channels (here, OmpE and NavAb were chosen). This study provides a novel approach to obtain advanced artificial CNT-based nanopores. Firstly, the ''design principles'' learned from nature are tabulated, then these principles are validated and optimized by computer simulation, and finally the principles are employed to design CNT-based materials. The size regime (nanometer-size of channels, also called nanoconfinement) is the integral parameter of CNTs, which seriously affects the transport of ions, water, and biomolecules. A smaller size has a great impact on fast, nearly friction-less flux water flow (flowing in single-file water type) and unusual ion selectivity (Fig. 3b).[89,114,116] In a pore with the size of 1.5 nm under an applied electric field, two K^{+} cations (blue) rapidly pass through within ~2 ns, which is accompanied by the overall flow of water molecules (red) through the CNT channel. The electrostatic effects and strong electroosmotic coupling are supposed to cause these phenomena.

Carbon nanotube porins (CNTPs), a system in which short pieces of CNTs self-insert into the lipid bilayer, are the representative model for bioinspired CNT-based materials to truly mimic the biological membrane channels. In 2014, Noy *et al.* firstly established CNTPs.[117] Fig. 3c shows a simple prototype for a CNT-based system as artificial nanochannels under physiological conditions. In this system, small molecules are transported but large uncharged species are rejected because of the size exclusion (Fig. 3d). These rejection characteristics were governed by the mechanisms of the electrostatic repulsion and the Donnan membrane equilibrium.[118] Further studies showed that the rate of proton transport would be enhanced by an order of magnitude in the 0.8 nm-diameter CNTPs. This is quite different from that in the 1.5 nm-diameter CNTPs, where Ca^{2+} ions can modulate this proton conductance.[119] In 0.8-nanometer-diameter CNTPs, water molecules are forced into a single-chain configuration and anion transport is blocked even in the presence of salts. The tunable ion selectivity configured the CNTPs into the switchable ionic diodes.[67] It has also been reported that amphiphilic block copolymers were utilized as lipid bilayers when combining CNTs to get a fully synthetic biomimetic membrane, where they still maintained high proton and water permeability and had an additional response to osmotic stress within the robust polymersomes (Fig. 3e).[120] In conclusion, these CNTPs exploit the unique structure of CNTs with suitable biomimetic nanochannels and selective mass transport performances, which brilliantly present insights to extend the applications of bioinspired CNT-based nanochannel materials in novel biomimetic systems.

To date, SWCNTs are widely understood as transporters of electronic current, electrolyte, and ions, where they act as synthetic ion channels. Integrating ion transistors and electron transistors in devices can provide SWCNT-based bionic materials with breakthrough performances in mass transport. As shown in Fig. 3f, Shepard *et al.* demonstrated an electrically actuated, CNT-based biomimetic ion pump with the ability to simultaneously transport electrons and nanofluids in a single SWCNT device.[121] The Coulomb drag effect was engineered in this SWCNT device, which realized electrolyte transport without a potential difference and pressure gradient. In addition, chemically modified or doped CNTs have emerged, breaking the limitation that bioinspired CNT-based materials are not sufficient to satisfy diverse specific demands in real-life applications.[122] Highly efficient electroosmotic flow was observed in Hinds' lab by functionalizing a surface with a pre-microtome vertically aligned CNT-epoxy composite.[123,124] One recent study in Hou's lab demonstrated another method of reversible ion transport control. The system was fabricated using a CNT array-polydimethylsiloxane composite.[125] As shown in Fig. 3g, ionic rectification could be adjusted in real time by dynamically changing the channel curvature.

In conclusion, we summarized the following development characteristics of CNTs as artificial nanochannels in bioinspired CNT-based materials in the past 5 years. (1) Computational chemistry has been widely used to guide the design of new CNT-based materials for mass transport in nano-confined channels. (2) Novel systems such as the emergence of CNTPs, which have identical and even exceptional bio-molecule permeability properties. (3) Various methods, such as integrating ionic and electronic transistors with SWCNTs, chemically modifying or doping CNTs in aligned CNT-polymer composites, and controlling the curvature of CNTs, causing CNT-based material systems to have unique mass transport behaviors, which can be applied in numerous fields ranging from biosensing and nanofluidics to filtration.

3.2 As construction materials

3.2.1 CNT-assembled structures. To achieve the best use of the structural superiority of CNTs, in some design strategies for bioinspired CNT-based materials, CNTs are usually assembled or arranged in particular structures. In one strategy, individual CNTs are employed to mimic the ''stem'' and the ''branches'' of plants. The novel ear-of-wheat-shape CNT-based electrode material is shown in Fig. 4a,[104] while manganese oxide (Mn_3O_4) nanoparticles (MONPs) (''cereal-grains'') are tightly anchored on the surface of CNTs (''central stems''). The metal oxide Mn_3O_4 has a high theoretical potential for lithium storage through conversion reactions. When accompanied by CNTs, its defect of low conductivity is further addressed, resulting in a high reversible capacity.

Carbon nanotube fibers (CNT fibers) and CNT yarns are almost identical assembly types of CNT-based materials in bioinspired design, which are famous for overcoming the length limitation of individual CNTs, possessing a length of up to several kilometers. However, the breaking strength of individual CNTs generally decreases when they are assembled into structures similar to CNT-based fibers or yarn materials. The weak van der Waals forces in adjacent nanotubes are the key factor in this limitation. One approach learned from nature is to enhance the mechanical strength by introducing stronger interactions between neighboring CNTs. The design inspirations come from natural masterpieces including silk and muscles,

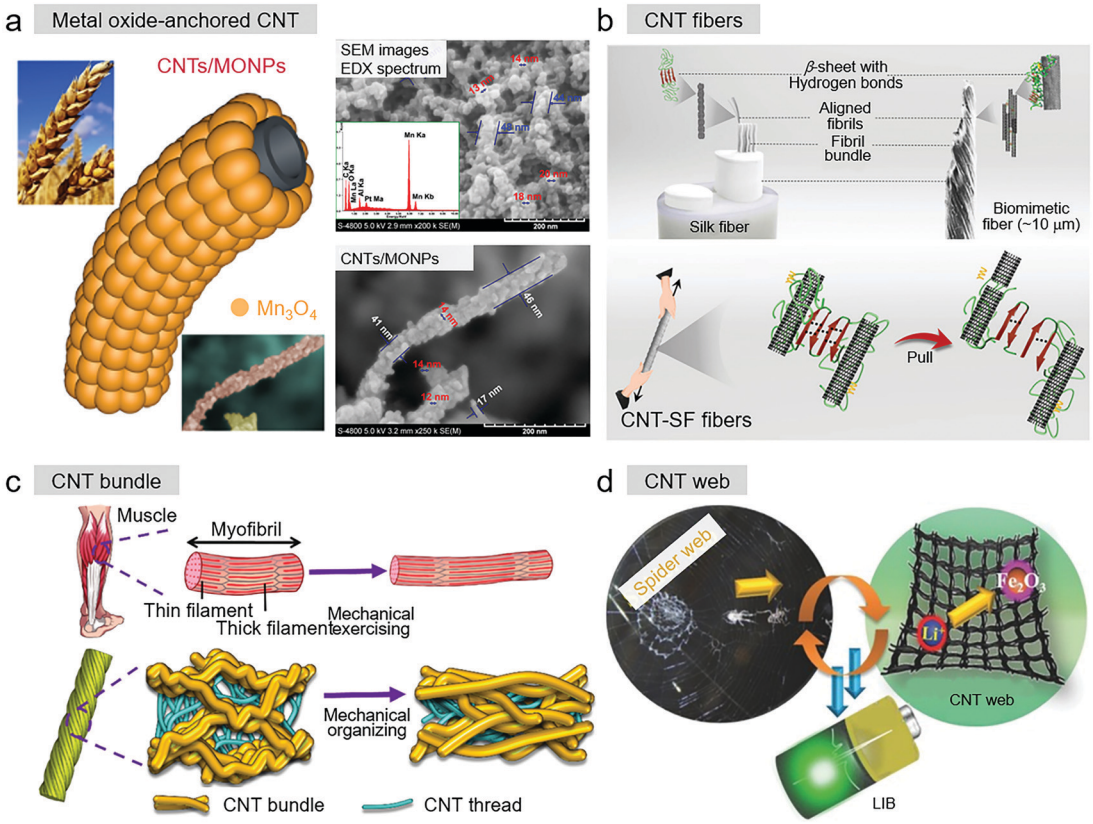

Fig. 4 (a) Biomimetic ear-of-wheat-shaped Mn_3O_4 nanoparticles on CNTs. Reproduced with permission.[104] Copyright 2020, Wiley-VCH. (b) Biomimetic CNT-SF fiber and its breaking process. Reproduced with permission.[94] Copyright 2021, Wiley-VCH. (c) Bioinspired microstructure-reorganized behavior of CNT yarn. Reproduced with permission.[95] Copyright 2020, The Royal Society of Chemistry. (d) Biomimetic spider-web-like MWCNT/γ-Fe_2O_3 composites. Reproduced with permission.[101] Copyright 2017, Wiley-VCH.

which have hierarchical structures and possess excellent mechanical properties. Learning from the biological structures of natural silk fibers, reinforcing strategies of interactions force replacement and inorganic–organic interfacial design were developed.[126] Mimicking silk fibers, Zhang *et al.* injected silk fibroin (SF) and glycerol into spun CNT fibers and obtained composite CNT-based fibers (Fig. 4b), showing an increased breaking strength of up to 1023 MPa (+250%), improved toughness from 7.8 to 10.3 MJ m^{-3} (+132%), and Young's modulus of 81.3 GPa (+442%).[94] The MD simulation indicated that the glycerol-rich β-sheet of SF together with abundant hydrogen bonds between SF and CNTs contributed to enhancing the mechanical properties of the CNT fibers. To construct the assembled CNT yarns with higher mechanical properties, inspired by the mechanical exercising-induced hierarchical structure of human muscles, through cyclic stretching training (cyclic stretching or cyclic loading), Xu *et al.* firstly created a novel microstructure-reorganized strategy to fabricate a hierarchical CNT bundle and CNT thread mechanical organizing structure (Fig. 4c).[95] This structure entirely copied the structural organization behavior of human muscles and had +64% tensile strength, +148% Young's modulus, +30% conductivity, and +35% enhanced piezo-resistive sensitivity than that of the pristine CNT yarn.

The spider with a web-like shape structure is another bioinspired design strategy for bioinspired CNT-based materials with particular structures of CNT web. As shown in Fig. 4d, to improve the cell performance, a method of controlling the structure and composition of the anode materials was conducted, where a material with biomimetic spider-web-like MWCNT networks was demonstrated by Park *et al.*, which had the structural characteristic and working patterns of sticky spider-webs.[101] In this system, the MWCNT web functioned as the conductive support with 3D internetworked pathways to improve the percolated transport, and γ-Fe_2O_3 particles as the active sites tightly attached on the surface of the MWCNT network to make the construction more stable. Ultimately the obtained biomimetic LIB exhibited a high capacity of 822 mA h g^{-1} at 0.05 A g^{-1} with a fast rate capability of 72.3% retention at a current density in the range of 0.05 to 1 A g^{-1}, and promising cycling stability (>88% retention after 310 cycles with >99% Coulombic efficiency).

Geckos, with extraordinary adherence and climbing ability on diverse surfaces in various atmospheres, have fascinated humans for millennia. Utilizing modern micro-nano morphological imaging techniques (SEM, TEM, and AFM), the secret of their climbing mechanism has been partly revealed. The van der Waals forces from the spatula of the geckos' feet with a hierarchical structure are considered as the origin of their adhesion. Accordingly,

inspired by the biological structure of geckos' feet, various fabrication strategies have been developed to create synthetic dry adhesive surfaces. Among the adopted materials, the vertically aligned CNTs (VA-CNTs) are outstanding because of their remarkable mechanical properties, large aspect ratio, and exceptional alignment type by just abundant hollow individual CNTs *via* horizontal van der Waals interactions. Theoretical simulation has predicted that their adhesion strength is up to 500 N cm^{-2} on glass, which is much higher that of the natural array on geckos' feet.

Surface modification is an efficient strategy to directly enhance the adhesion of contact surfaces. Dai *et al.* proved that the best adhesion strength of 29.3 N cm^{-2} could be achieved just by using radio-frequency tetrafluoromethane plasma.[127] Also, polydopamine (PDA) in the mussel adhesive protein is considered the crucial component in simple, convenient, efficient, and environmentally friendly chemical modification, which can help improve the dry adhesion performance of traditional biomimetic CNT-based materials, even in a wet environment (Fig. 5a).[105] Patterning CNTs is another useful strategy. Recently, Yao *et al.* reported the one-step synthesis of a CNT forest (CNTF) (Fig. 5b).[128] In this system, the patterned aluminum layer controlled the morphology formation of CNTs to form CNTF, which resulted in a 5.9-times increase in adhesion.

3.2.2 CNT composites. To make full use of the structural, surficial, and conductive properties of CNTs, they are adopted as multifunctional nano-scale fillers to create composite structures in most design strategies for bioinspired CNT-based materials. Normally, the accompanying materials are inorganic, organic, and polymer materials. There are three main design types of bioinspired CNT-based composites including CNT-polymer composites, CNT layer-by-layer composites, and CNT hydrogels.

To obtain bioinspired CNT-based materials with particular requirements such as softness, wearability, and flexibility, polymers are added. As shown in Fig. 6a, with a spring-like structure, s superelastic and electroconductive fiber was fabricated by Xu *et al.*[73] By imitating the behavior of climbing plants, this fiber possessed biomimetic coiled tendril structures. Elastic polyester fiber (PF) was chosen as the core yarn, and flexible but conductive CNT/PDMS composite yarn (C/P CY) was then wrapped around PF to produce C/P CWY. CNTs constituted the framework and the coiled C/P CY provided abundant conductive pathways.

The polar bear pelt has an impressive radiation control strategy. Mimicking this strategy, Qiu *et al.* recently used a multistep to design a porous Ag/cellulose/CNT-laminated nanofiber membrane (Fig. 6b).[110] This membrane had a laminated construction, where the CNT layer coating the cellulose layer was the solar radiation absorptivity layer to harvest solar thermal energy. An Ag layer was deposited *via* magnetron sputtering on the other side of the cellulose layer, reflecting infrared radiation from the human body. CNTs are black materials, and thus the obtained CNT layer could function as a heat collector to maximize heat input from the sun, while the Ag layer acted as the infrared reflector to minimize the human radiation heat output. Using the electrical conductivity of the additive CNTs to generate Joule heat, the membrane also had perfect thermal management.

Good conductivity is one advantage of CNTs, making bioinspired CNT-based materials excellent candidates in the field of energy conversion. Mimicking entire bulk structures to form sheet materials or composites with multidimensional pores is one design strategy. As shown in Fig. 6c, Yang *et al.* developed an ordered nacre-like cathode for Li–S batteries.[102] A high sulfur loading was achieved with conductive polyvinylpyrrolidone (PVP) dispersed CNT-based monolith structures, in which the interval interspace was prepared *via* a unidirectional freeze-drying method. This nacre structure-like CNT sheet matrix resulted in cyclic stability with >99.9% coulombic efficiency and outstanding rate performance with 5 mg cm^{-2} sulfur loading, further increasing to 10 mg cm^{-2}, high discharging capacity of 1236 mA h g^{-1} at 0.1C and 498 mA h g^{-1} at 2C.

Interestingly, design strategies by controlling the alignment of CNTs within polymers for the fabrication of bioinspired CNT-based materials with additional properties have also attracted attention from researchers. Through an electrically assisted 3D printing method, Chen *et al.* fabricated Menger structures with Bouligand-type surface-modified MECNTs (MWCNT-S) to recreate the architectures of the claws of *Homarus americanus* (which are mainly are made of Bouligand-type chitin-protein fibers).[108] In the printing process, controlling the rotating electrical field could dynamically align the MWCNTs. A smaller rotation angle of adjacent MWCNTs led to greater energy dissipation and impact resistance. Moreover, with the requirement of multifunctional

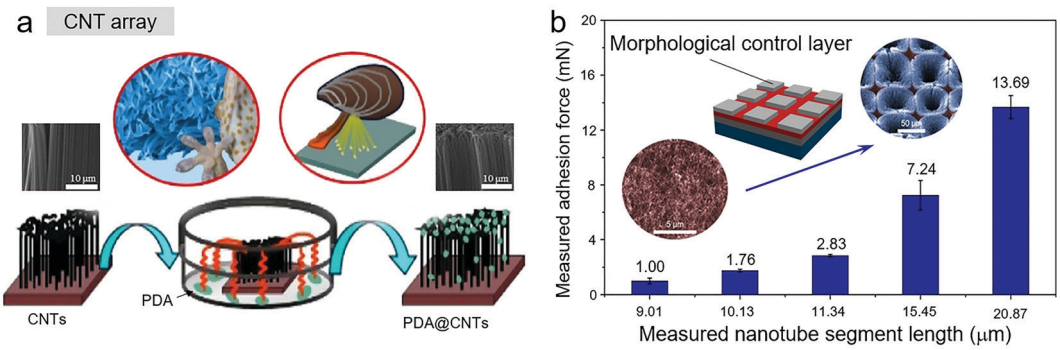

Fig. 5 (a) Fabrication of PDA-modified VA-CNTs. Reproduced with permission.[105] Copyright 2019, the American Chemical Society. (b) Horizontally aligned surface segments, enhancing the adhesion of CNTF. Reproduced with permission.[128] Copyright 2021, Elsevier.

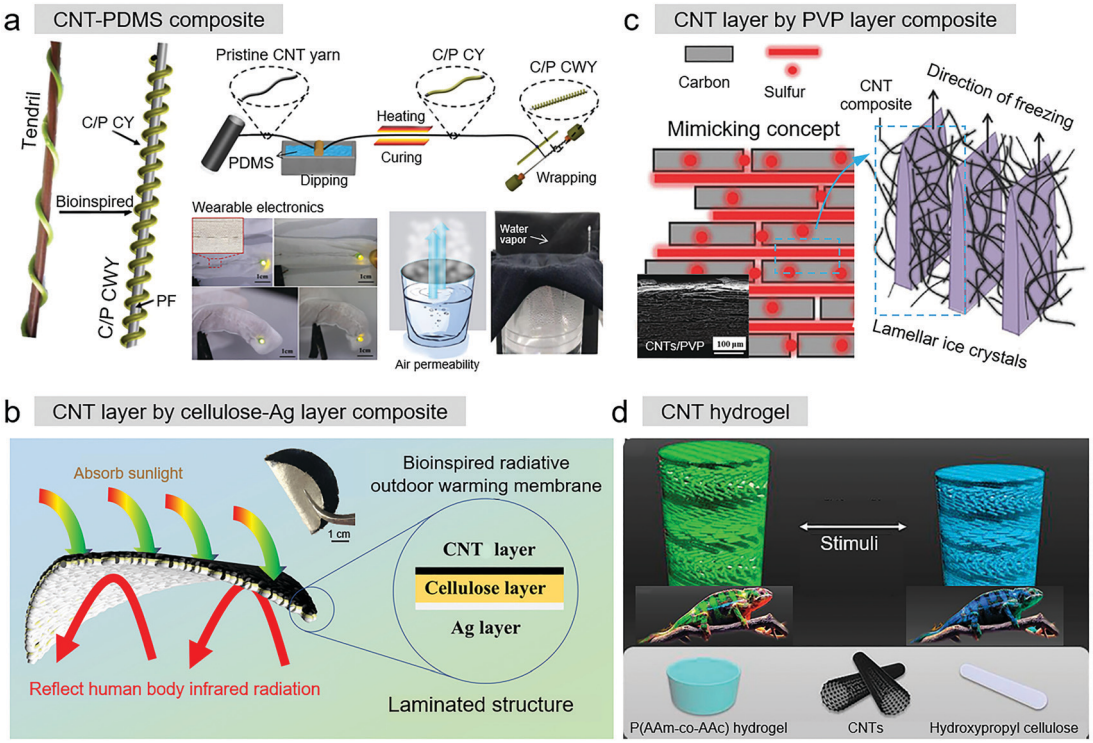

Fig. 6 (a) Bioinspired superelastic E-fiber for wearable electronics. Reproduced with permission.[73] Copyright 2019, American Chemical Society. (b) Porous Ag/cellulose/CNT-laminated nanofiber membrane. Reproduced with permission.[110] Copyright 2020, American Chemical Society. (c) Nacre-like CNTs sheet. Reproduced with permission.[102] Copyright 2018, Wiley-VCH. (d) Conductive CNT-based cellulose structural color hydrogel. Reproduced with permission.[107] Copyright 2020, National Academy of Sciences.

bionic electronic skins for smartly outputting multi-stimulation signals, inspired by the chameleon, Zhao *et al.* presented a multifunctional E-skin composited liquid-crystal hydrogel based on poly(acrylamide-*co*-acrylic acid) hydrogel (PACA), CNTs, and hydroxypropyl cellulose (HPC) (shown in Fig. 6d).[107] With the help of additive CNTs in this system, the composite with hydrogel structure could output stimuli in electrical resistance signals. Based on a variation in color, the multifunctional bioinspired CNT-based materials had the ability to visually map the stimulating sites and quantitatively feedback external stimuli with electrical resistance changes.

Various methods, such as solvent casting, melt mixing method, and *in situ* polymerization have been adopted to obtain stable CNT-based composites.[129] Naturally, CNTs are hydrophobic, possibly having toxicity by inducing an immune response in clinical applications.[18,25] Accordingly, functionalized CNTs (*e.g.*, carboxylic, carbonyl, and hydroxyl groups) or CNT compositions (*e.g.*, tetrafluoromethane, polydopamine, and tannic acid) are fabricated by introducing molecules with hydrophilic, bioactive or specific groups, improving the dispersion of CNTs and the adhesion between CNTs and accompanying materials.[85,97,105,127,130,131]

4. Applications

The superiorities of CNTs and informed design strategies enable material engineers to fabricate bioinspired CNT-based materials, with design ideas from nature that are both ingenious and practical, which have beneficial applications. In this section, we demonstrate a few typical application examples of bioinspired CNT-based materials.

4.1 Reinforcement materials

Reinforcement materials emerged in the middle of 20th century. Their promising characteristics of high stiffness, toughness with lightweight, and anticorrosion, make them applicable in aerospace, constriction, energy generators, biomedicine, *etc.* However, although single CNTs have the strongest intrinsic mechanical properties, the average strength of an individual CNT is only 9.6 GPa in CNT-based materials. Thus, efforts are still needed to change the weak interaction between two neighboring CNTs for the wide use of CNTs as construction materials. Bioinspired CNT-based materials, with homologous reinforcing strategies from nature, will profoundly make bioinspired CNT-based materials suitable as reinforcement materials.

In Section 2, we discussed the bioinspired CNT-based reinforcement materials with enhanced mechanical properties of CNT fibers, CNT yarn, and CNT web structures. Moreover, inspired by the special hierarchical structure of natural spider silk, Pan *et al.* fabricated bioinspired spider silk single-walled carbon nanotubes (BISS-SWCNTs) (Fig. 7a).[69] Through a multi-step fabrication procedure, the internal and external structures of these CNT-based film materials had similar appearances to that of spider silk. Specially, iron particles were embedded in BISS-SWCNT bundles as glue spots, and the highly organized

SWCNTs with a skin-core structure were surrounded by an amorphous carbon layer. This bioinspired material exhibited a tensile strength of 550 MPa and Young's modulus of 6.5 GPa. Due to the above-mentioned hierarchical structure, the reinforcement was isotropic in the transformation of BISS-SWCNTs to alignment. Further equivalent superiority mechanical properties were observed in experiments on the PMMA/BISS-SWCNT/PMMA composite film, which had 300% improvement in tensile strength and 300% improvement in Young's modulus.

To obtain bio-based nanocomposites with flexible and stretchable abilities of high strength and toughness, learning from the interface engineering of mussel byssus, Li *et al.* described a biomimetic design strategy for the fabrication of TEMPO-oxidized nanofibrillated cellulose (TONFC)/soy protein isolate (SPI) (SPI/CT/TONFC, SCTs) nanocomposite films with strong and tough mechanical properties (Fig. 7b).[97] Tannic acid-functionalized MWCNTs (PCT) were employed as cross-linkers with high functionality in the system, constructing a synergistic and sacrificial metal–ligand bonding interface between PCT and TONFC with Fe(III) mediation. The nanocomposite films exhibited a tensile strength of 11.5 MPa, toughness of 6.9 MJ m^{-3}, elongation of 79.3%, and high electrical conductivity and good water resistance.

The direct mixture of CNTs and polymers, as one simple and cost effective method, is broadly employed to fabricate CNT-based structural materials with enhanced mechanical behavior. Nacre has extraordinary strength and toughness, relying on a brick-and-mortar architecture, also providing the possibility of creating polymer composites to obtain high-performance CNT-based reinforcement materials. Accordingly, Zhong *et al.* designed nacre-mimetic CNT@polyaniline/graphene oxide/biomass tannin (CNT@PANI/rGO/TA) (Fig. 7c). Biomass tannin (TA) was used as the glue, and together with "mortar" polyaniline, wrapped carbon nanotubes (CNT@PANI) to stick the reduced rGO "bricks" together.[99] This bioinspired material exhibited high mechanical strength of 174.6 MPa and toughness of 9.17 MJ m^{-3}. Similarly, individual CNTs (with the configuration of 1D fibers) were regarded as the "mortar" to link rGO to obtain CNT/rGO materials. Their tensile strength also improved to 106.2 ± 5.5 MPa and the toughness was 2.27 ± 0.4 MJ m^{-3}.

Mimicking the *Salvinia molesta* superhydrophobic leaf structure *via* immersed surface accumulation (ISA) 3D printing, Chen *et al.* fabricated superhydrophobic micro-scale eggbeaters (Fig. 7d). MWCNTs, which ultimately enhanced the mechanical strength and surface roughness of the solidified microstructures, were initially added to photocurable resin.[83] Consequently, stable 3D printed hairs were achieved and suspended eggbeaters, which did not collapse or adhere together, were obtained. After the addition of 0.5 wt% MWCNTs, the modulus of the structure increased from 161 to 455 MPa, while superhydrophobicity was obtained. With an increase in the MWCNT content, the surface roughness also increased.

4.2 Energy conversion

CNTs, serving as stable frameworks and substrates in bioinspired CNT-based materials, offer the feature of high electrical conductivity. Meanwhile, the interlinked micro/nano network and appropriate

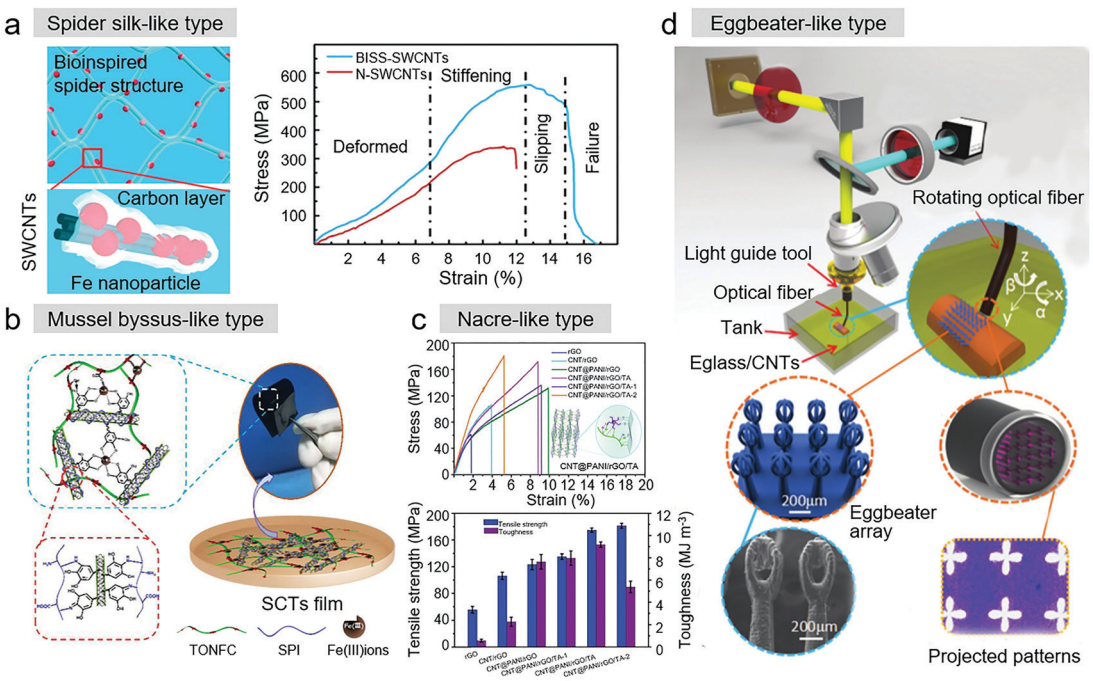

Fig. 7 (a) With a similar spider silk-like structure, the bioinspired BISS-SWCNTs had ultrahigh mechanical properties. Reproduced with permission.[69] Copyright 2016, the American Chemical Society. (b) SCT nanocomposite film. Reproduced with permission.[97] Copyright 2017, Elsevier. (c) CNT@PANI/rGO/TA composite. Reproduced with permission.[99] Copyright 2021, The Royal Society of Chemistry. (d) Optical system in the ISA-3D printing process for 3D-printed biomimetic super-hydrophobic structure. Reproduced with permission.[83] Copyright 2017, Wiley-VCH.

porosity from the compositing structure also prolong the conductive pathway of materials by increasing their ion transportation ability. These behaviors have important implications for the application of bioinspired CNT-based materials in energy conversion.

Tin phosphide (Sn_4P_3), a metal phosphide, is a potential anode material in sodium-ion batteries (SIBs). However, in the Sn_4P_3 sodiation process, its low ionic and electronic conductivity lead to large volume expansion, limiting its utilization in SIBs. Recently, Knibbe *et al.* reported a stem-like CNT-based bioinspired material, where fructus-like Sn_4P_3 nanoparticles were anchored on the surface of CNTs through hydrothermal reaction followed by thermal treatment (Fig. 8a).[92] With this biomimetic structure, the SIB achieved a superior electrochemical performance, with a high capacity of 742 mA h g^{-1} at 0.2C after 150 cycles and a superior rate of 449 mA h g^{-1} at 2C after 500 cycles.

TiO_2, due to its high economic value, environment friendly nature, and chemical inertness, has been the prevailing photocatalytic material, but its application is limited because of its ineffective solar energy conversion and fast electron–hole recombination rate. Zheng *et al.* proved that the combination of TiO_2 and CNT composites with structures inspired by trees (Fig. 8b) is an effective way to realize direct electron transport, and photocatalysis was enhanced due to the larger specific surface and thermoelectric conductivity of CNTs.[57]

Recently, Miao *et al.* was inspired by the hierarchical microchannel structure of wood to develop a CNT-participated nanofibrous organic cathode. This cathode consisted of PTCDA/nitrogen-doped carbon/carbon nanotubes (PTCDA/NC/CNTs), as shown in Fig. 8c.[89] In the SIBs, this bioinspired CNT-based composite cathode had ultra-strong capillarity, highly reversible capacity, excellent rate performance, and ultra-long cyclic stability. As a conductive agent for rapid electron transfer, CNTs were employed to construct 3D interconnected conductive frameworks through electrospinning. PTCDA/NC/CNTs exhibited rapid ionic/electronic transport, high diffusion coefficients of Na^+ and ultrafast reaction kinetics due to the rigid hollow nanostructure of CNTs, which formed a superb capillary. Moreover, bioinspired CNT-based nanomaterials have the advantages of good optical adsorption and free water transport, which make them promising for efficient solar steam generation. Zhu *et al.* fabricated a direct solar steam generation system with inspiration from the evaporation of sweat on the human skin and the transpiration in plants in biological systems.[98] Utilizing these CNT films as floating photo-thermal collectors, the enhanced steam generation rate of 3.615 kg m^{-2} h^{-1} and >40% evaporation efficiency were achieved under 5 times solar intensity.

4.3 Nanopatterned surfaces

Besides their potential as reinforcing materials with high mechanical strength and chemical stability, the unique nanoscale morphology, low hydrophilicity, and optical characteristics of assembled structures of CNTs are also instructive for the

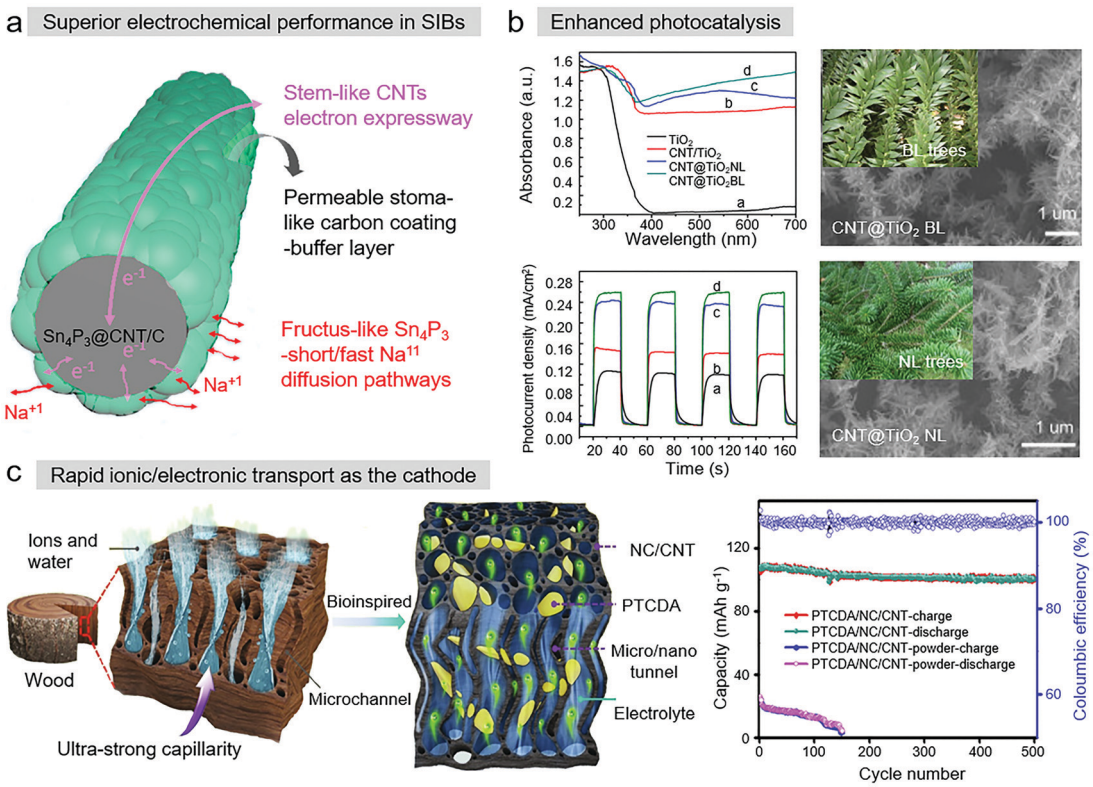

Fig. 8 (a) Biomimetic Sn_4P_3 anchored on CNTs. Reproduced with permission.[103] Copyright 2020, the American Chemical Society. (b) Biomimetic CNT@TiO_2 composite. Reproduced with permission.[68] Copyright 2015, Elsevier. (c) Design concept of the PTCDA/NC/CNT electrode. Reproduced with permission.[100] Copyright 2020, Elsevier.

application of bioinspired CNT-based materials in nanopatterned surfaces.[132,133] Liz-Marzán *et al.* reported classical sea-anemone-like CNT-based hollow capsules with magnetic and reinforced properties. The CNT-coated Fe_3O_4 NP@PS spheres were used as the "hair" to provide the reinforcement.[49] This outer surface structure is not only conductive to the controllable deposition of SiO_2, but also stable in the washing process of the PS template. Interestingly, changing the length of CNTs would control the modification surface of the capsules, resulting in more complex structures with multi-level branching. The low hydrophilicity and chemical stability of CNTs are also beneficial in the design of surfaces with anti-fouling and anti-corrosion performances using bioinspired CNT-based materials. By incorporating the mussel-inspired material PDA, Yu *et al.* fabricated a PDA@CNT/PU nanofiber membrane, which exhibited superhydrophilicity and underwater superoleophobicity.[134] Mimicking the micro-sphere/nano-thorn surface structure of the golden spherical cactus, Zhu *et al.* fabricated a superhydrophobic polysulfone (PSU)/CNT nanocomposite (Fig. 9a).[72] These superhydrophobic materials could be deposited on various substrates just by electrostatic powder spraying, resulting in surfaces possessing a water contact angle greater than $164^\circ \pm 1.5^\circ$, sliding angle as low as $5^\circ \pm 0.5^\circ$, and self-cleaning ability and anti-corrosion in strong acid, alkaline and NaCl solutions. Recently, inspired by an arachnid, Li *et al.* developed a one-step thermal chemical vapor deposition method to fabricate a CNT stainless steel mesh (CNT@SSM) membrane (Fig. 9b). This membrane possessed excellent superhydrophilic and underwater-superoleophobic and anti-fouling properties.[135] These salient surfaces in bioinspired CNT-based materials can further expand their application scope to hazardous water treatment.

Additive CNTs on surfaces also have a contribution to enhanced color saturation. CNTs are ultra-black materials with a low theoretical effective index (n_{eff} = 1.01–1.10), stemming from their internal structures. Learning from the moth-eye effect, Motta *et al.* fabricated an optical film with SWCNT coating-deposited Si, which realized omnidirectional, broad-band, and nearly polarization-independent suppression.[111] With the technology of coating optical films on arbitrary substrates, the optical absorption and emission properties of the devices were improved.

4.4 Dry adhesion

Although VA-CNTs have been proven to be suitable artificial materials for the fabrication of dry adhesive materials in theory, they still have a long way to go. To obtain the VA-CNT materials with extraordinary adhesive performances, surface modification of CNTs and patterned CNT arrays have been developed (seen in Section 3). The aim is to achieve a simple but high-efficiency procedure to obtain a perfect dry adhesive surface.

Numerous bioinspired VA-CNT-based materials have been fabricated by mimicking the structures of geckos' feet, but the design principles and synthetic mechanisms of how CNT arrays lead to dry adhesion and the key factors to enhance their performances remain unclear. In recent years, researchers have gradually focused on the influence of the key parameters in the fabrication process. Firstly, the packing density of VA-CNTs and the roughness of the surface were explored. With a high density, there was no adhesion. With an increase in roughness, the adhesion increased obviously, but the shear direction adhesion decreased (Fig. 10a).[136] Gorb *et al.* discussed the tribological properties of densely aligned VA-CNTs with a synthetic length of up to 1.1 mm.[138] A high coefficient of friction, μ, of 5–6 was showed in the initial sliding cycles, which then decreased to 2–3 in fourth and fifth cycles. The applied shear force inducing a strong contribution of adhesion was the main reason. One study showed that the incorporation of Fe and Al_2O_3 layers had a synergistic effect on the growth of structures and morphologies of VA-CNT materials, such as orientation, density, diameter, and growth rate (Fig. 10b).[137] Conversely, the adhesion could be controlled with a change in these layers. Another study concentrated on the relation between the adhesion force of VA-CNTs and their mechanical behaviors.[139] It indicated that the 3.4% higher fraction of VA-CNT arrays resulted in no adhesion effect, while at low density (less than 0.5%), the adhesion performance was strongly associated with plastic deformation. Mechanical compliance in the area near the contact interfaces may be the dominant factor.

It is worth noting that although VA-CNT materials have been utilized in bioinspired dry adhesion for no more than 20 years, their dry adhesion performances have been greatly improved. CNT-based array materials are superior to the natural geckos'

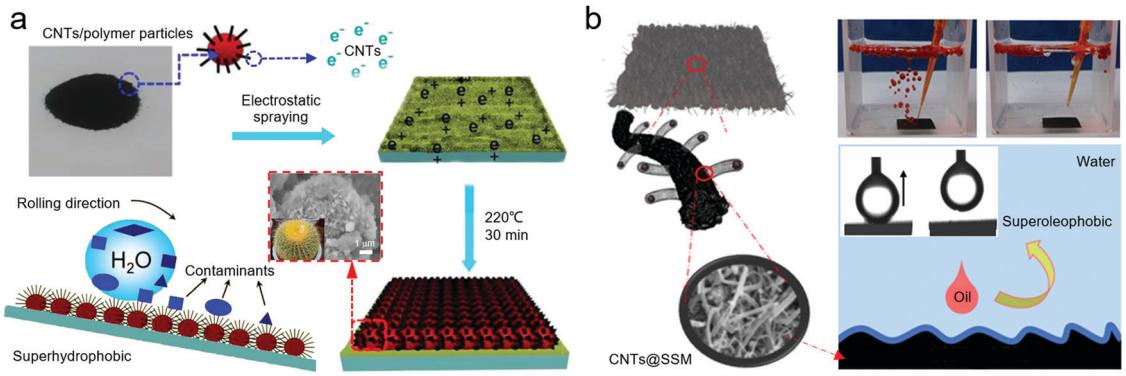

Fig. 9 (a) Biomimetic spherical cactus superhydrophobic (PSU)/CNT coating. Reproduced with permission.[72] Copyright 2018, Elsevier. (b) CNT@SSM membrane. Reproduced with permission.[135] Copyright 2021, Elsevier.

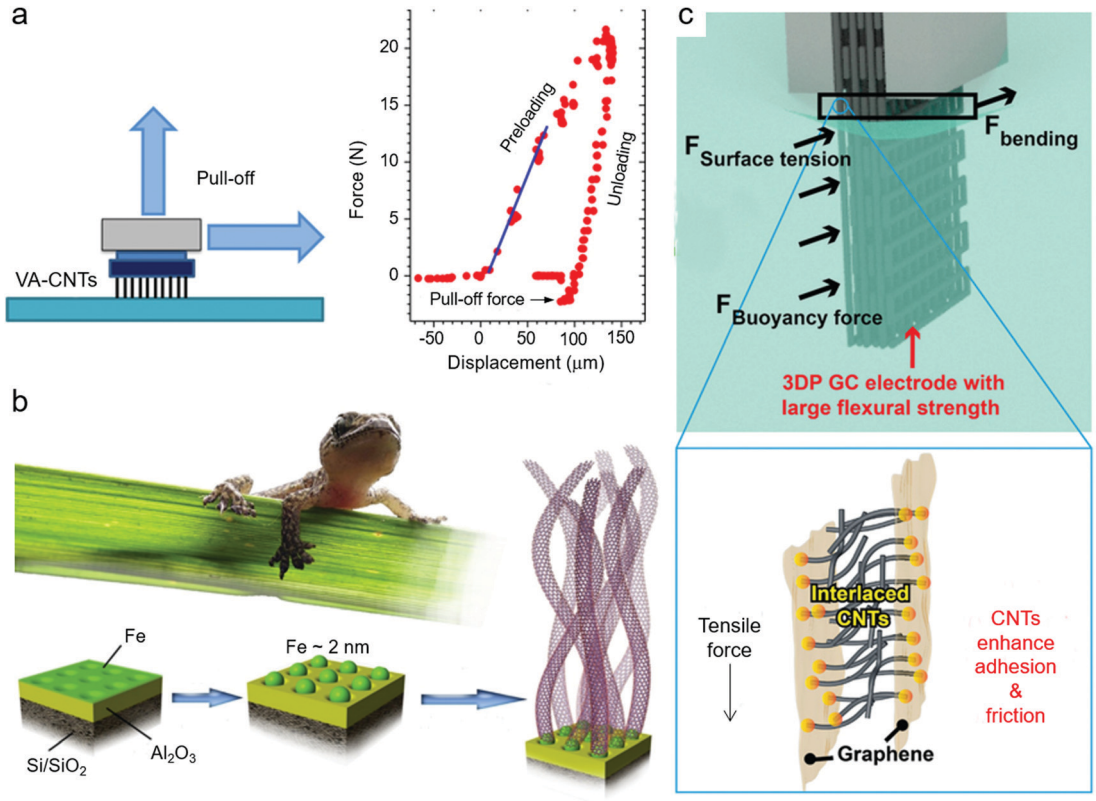

Fig. 10 (a) Effects of packing density and surface roughness on adhesion of VA-CNTs. Reproduced with permission.[136] Copyright 2015, the American Chemical Society. (b) Synergistic effects of Fe and Al_2O_3 layers on the growth of VA-CNTs. Reproduced with permission.[137] Copyright 2018, Elsevier. (c) Gecko's feet-inspired design of 3DP GC electrode. Reproduced with permission.[106] Copyright 2020, Wiley-VCH.

feet. However, big breakthroughs have been less frequent in recent years, and some exclusive obstacles still remain to be solved. It is necessary to move back and deeply delve into the basic principles of gecko adhesion. One reason is that geckos have a lot of natural adhesion systems that are not completely known well. Innovative applications corresponding to the dry adhesion behaviors are also urgent. One good start may be the study by Jiang *et al.*, who reported a 3D-printed bioinspired electrode of graphene/CNTs (3DP GC) (Fig. 10c).[106] Mimicking the geckos' feet, the obtained electrode processed a hierarchical porous structure with high flexural strength of 96.2 kPa. Increasing the friction and adhesion in the neighboring 2D graphene nanosheets, the 1D CNTs played a critical role in the enhanced flexural strength.

4.5 Bioengineering

Depending on the electrical conductivity of CNTs and decorated biofunctional groups on their surface, bioinspired CNT-based materials can monitor molecular recognition and transformation processes, which broaden their applications in biosensing and biocatalysis. Swager *et al.* reported the fabrication of a chemiresistive glucose sensor based on poly-(4-vinylpyridine) (P4VP) and SWCNT composites (Fig. 11a).[140] A biomimetic surface was obtained in the system by cooperation with glucose oxidase (GOx). This biomimetic glucose sensor displayed a decrease in electrical resistance to exhibit high selectivity and instant response (within 3 s) to glucose. In another biomimetic oxidase sensor system, iron porphyrins, a type of horseradish peroxidase, were immobilized on modified MWCNTs. This sensor was proven to be a simple, economical, and efficient method to detect catechol.[141] Zhang *et al.* firstly utilized a peptide as a DNA sensing element and built a novel CNT-DNA thin-film-transistor sensor.[142] Different from the former known DNA bio-detector and NanoDrop, this bio-inspired sensor had a broader sensing range of 1.6×10^{-4} to 5×10^{-6} M (the detection limit was 0.88 μg L^{-1}). In 2015, Wang *et al.* firstly found that carboxyl-functionalized SWCNHs (SWCNHs-COOH) had peroxidase-like activity similar to natural peroxidase. Even under harsh reaction conditions, SWCNHs-COOH was stable and exhibited high catalytic activity, which is regarded as a potential enzymatic mimic.[143] In recent years, a series of CNTs and their derivatives have emerged as highly efficient biocatalysts to mimic the function of biological enzymes, but their use is hampered by their unsatisfactory enzymatic efficiency. The accurate influence of various oxygenated groups on the surface of oxygenated group-enriched CNTs (*o*-CNTs) was firstly explored, including carbonyl, carboxyl, and hydroxyl groups (Fig. 11b).[144] The "competitive inhibition" mechanism was proposed. When weakening the noncatalytic sites, the catalytic efficiency of *o*-CNTs can be greatly improved. Once the surfaces of CNTs are well functionalized, both biocatalysis and biosensing can be achieved.

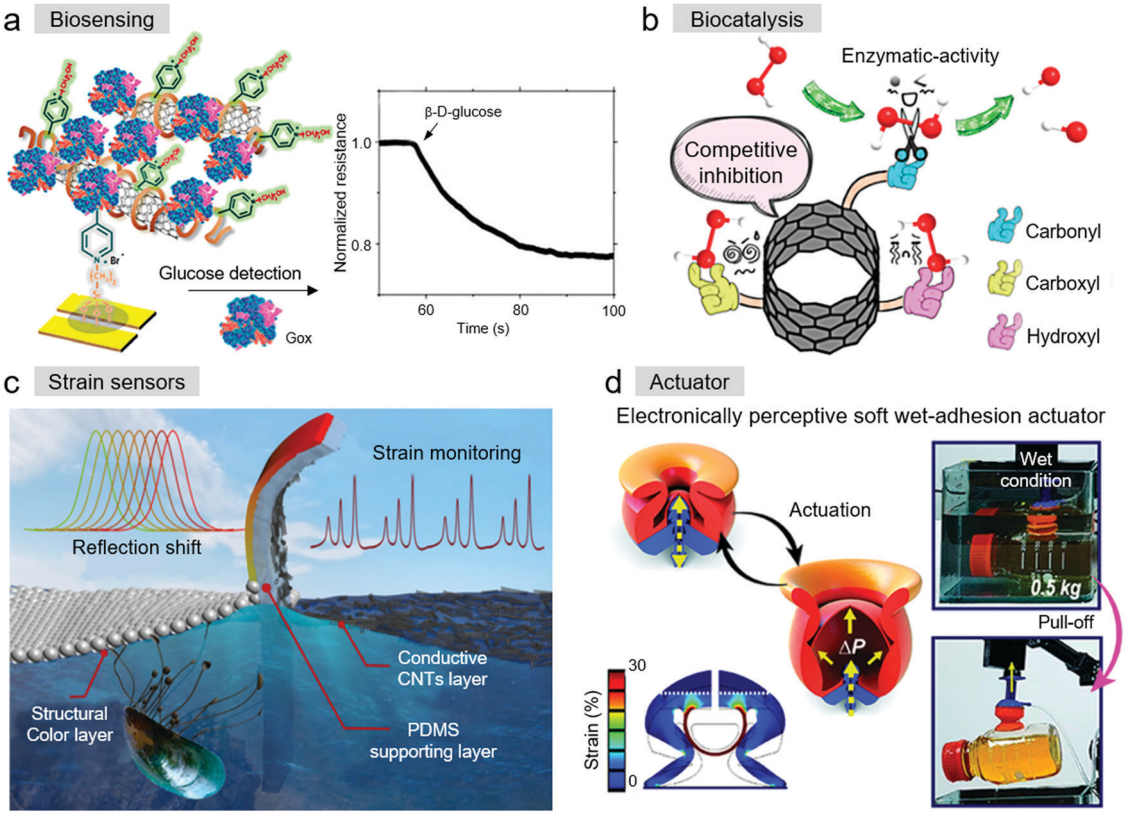

Fig. 11 (a) P4VP-SWCNT scaffolds for a chemiresistive glucose sensor. Reproduced with permission.[140] Copyright 2017, the American Chemical Society. (b) Peroxidase-like activity of *o*-CNTs. Reproduced with permission.[144] Copyright 2018, the American Chemical Society. (c) Bioinspired Janus structural color film as visually flexible electronics. Reproduced with permission.[146] Copyright 2021, Elsevier. (d) Electronic sensory soft adhesive actuator. Reproduced with permission.[74] Copyright 2021, the American Chemical Society.

In the study by Tang *et al.*, NiCoBP-MWCNT-conjugated anti-PSA antibody was fabricated.[145] For glucose oxidation, the nanocomplex exhibited outstanding catalytic behavior, and for detecting PSA, it also showed excellent performance simultaneously.

Bioinspired CNT-based materials have been widely used in electronics and actuators, which have particular requirements such as softness, wearability, and flexibility.[147–149] Mussel-inspired chemistry, which refers to the polymerization of the mussel-inspired material PDA, provides a simple but effective method for subsequent modification reactions or is utilized as a precursor for preparing functional CNT-based composite materials.[150] Learning from the anti-freezing/anti-heating performances in nature, Lu *et al.* developed an adhesive and conductive hydrogel using mussel chemistry.[96] In this system, PDA-decorated CNTs were dispersed in the hydrogel, and CNTs served as the nano reinforcements to enhance the conductive and mechanical properties. As shown in Fig. 11c, inspired by the structural color layer of mussels, a Janus structural color film was presented by Pan *et al.*, which had a conductive CNT-based layer, a supporting polydimethylsiloxane layer, and a structural color layer formed by 2D colloidal crystals (2D-CCs).[146] The experimental results indicated that these Janus structural color films exhibited stable electrical sensing and visualized color-sensing. Moreover, numerous specific sensors (*e.g.*, mechanical sensor,[151] wearable strain sensor,[152] temperature sensor,[153] and airflow sensor[154]) were developed *via* the methods of drop casting, air spraying, ultrasonic spraying, hybrid hydrogel, thermal mismatch design, *etc.* Besides, to obtain a device with the ability to catch objects with various shapes, inspired by the sensory grasping by the arm *of Octopus vulgaris*, Pang *et al.* recently fabricated an electronic sensory soft adhesive device (Fig. 11d).[74] CNT-based strain sensors, which served as the artificial octopus sucker, were placed on an irregular surface *via* a facile 3D spray coating process to the mimic nerve-like functions of the octopus. This strain sensors identified objects through patterns of strain distribution.

5. Conclusion and perspective

In the present review, we presented the progress on bioinspired CNT-based materials in recent years. CNTs exhibit superiors properties in the design of bioinspired CNT-based materials, such as unique hollow nanochannel structures, controllable functionalized surface, and tunable high conductivity. Benefiting from these special properties of CNTs, diverse design strategies for bioinspired CNT-based materials were introduced. The natural nanochannels of CNTs are an ideal model to study the mass transport behaviors in biological systems. Besides, CNTs are construction materials used to self-assemble or composite with other materials. Mimicking the structures of

natural plants, silk, muscles, spider webs, geckos' feet, *etc.*, bioinspired CNT-based materials have been fabricated with the CNT-assembled structures such as CNT fibers, CNT yarns, CNT web, and VA-CNT. Also, learning from tendrils, polar bears, nacre, chameleons, *etc.*, bioinspired CNT-based materials have been designed using CNT composites such as CNT-polymer composites, CNT layer-by-layer composites and CNT hydrogels. In addition, bioinspired CNT-based materials have shown significant applications in reinforcement materials, energy conversion, nanopatterned surfaces, dry adhesion, and bioengineering.

However, despite the substantial improvements, many challenges remain to be solved for bioinspired CNT-based materials. Firstly, in-depth exploration of the features and diversity of living organisms is required for achieving optimized bionic designs for CNT-based materials in both structure and function. Secondly, utilizing the unique structural, surficial, and conductive properties of CNTs as building blocks to design smart bioinspired CNT-based materials should be given exceptional attention. CNTs are easily produced, and their well-established functionalization methods can enlarge their diversity with multifunctions. Consequently, bioinspired CNT-based materials will be endowed with improved smart abilities, such as the ability to respond to heat, light, electricity, magnetism, specific molecules, *etc.* Thirdly, although bioinspired CNT-based materials have shown wide applications in some fields, further developments in their practical applications still have a long way to go. Overall, beyond the reported application fields, advances are anticipated in design strategies to obtain novel bioinspired CNT-based materials, feasibly leading to some burgeoning applications such as real-time virus detection, nanomaterial-based artificial synapses, and bioinspired nanofluidic iontronics.

Conflicts of interest

There are no conflicts of interest to declare.

Acknowledgements

This work was supported by the National Key R&D Program of China (2018YFA0209500), the National Natural Science Foundation of China (52025132, 21975209, 21621091 and 22021001), the Fundamental Research Funds for the Central Universities (20720190037 and 20720210056), and 111 Project (B16029).

References

1 Q. Cheng, J. Duan, Q. Zhang and L. Jiang, *ACS Nano*, 2015, **9**, 2231–2234.
2 N. S. Kumar, R. P. Suvarna, K. C. B. Naidu, P. Banerjee, A. Ratnamala and H. Manjunatha, *Appl. Phys. A: Mater. Sci. Process.*, 2020, **126**, 445–463.
3 J. J. Schneider, *Adv. Biosyst.*, 2017, **1**, 1700101.
4 D. Tasis, N. Tagmatarchis, A. Bianco and M. Prato, *Chem. Rev.*, 2006, **106**, 1105–1136.
5 J. K. Holt, H. G. Park, Y. M. Wang, M. Stadermann, A. B. Artyukhin, C. P. Grigoropoulos, A. Noy and O. Bakajin, *Science*, 2006, **312**, 1034–1037.
6 J. N. Coleman, U. Khan, W. J. Blau and Y. K. Gun'ko, *Carbon*, 2006, **44**, 1624–1652.
7 M. F. L. De Volder, S. H. Tawfick, R. H. Baughman and A. J. Hart, *Science*, 2013, **339**, 535–539.
8 M. Moniruzzaman and K. I. Winey, *Macromolecules*, 2006, **39**, 5194–5205.
9 L. Yan, X. Yang, Y. Zhao, Y. Wu, R. Motlhaletsi Moutloali, B. B. Mamba, P. Sorokin and L. Shao, *Sep. Purif. Technol.*, 2022, **285**, 120383.
10 M. S. Ganewatta, Z. K. Wang and C. B. Tang, *Nat. Rev. Chem.*, 2021, **5**, 753–772.
11 F. Lossada, D. Hoenders, J. Guo, D. Jiao and A. Walther, *Acc. Chem. Res.*, 2020, **53**, 2622–2635.
12 Z. L. Yu, B. Qin, Z. Y. Ma, Y. C. Gao, Q. F. Guan, H. B. Yang and S. H. Yu, *Adv. Mater.*, 2021, **33**, 2001086.
13 G. Liu, W. S. Y. Wong, M. Kraft, J. W. Ager, D. Vollmer and R. Xu, *Chem. Soc. Rev.*, 2021, **50**, 10674–10699.
14 Y. Hou and X. Hou, *Science*, 2021, **373**, 628–629.
15 A. B. Asha, Y. Chen and R. Narain, *Chem. Soc. Rev.*, 2021, **50**, 11668–11683.
16 Y. Li, *ACS Nano*, 2021, **15**, 9197–9200.
17 M. F. De Volder, S. H. Tawfick, R. H. Baughman and A. J. Hart, *Science*, 2013, **339**, 535–539.
18 B. Pei, W. Wang, N. Dunne and X. Li, *Nanomaterials*, 2019, **9**, 1501.
19 S. Iijima, *Nature*, 1991, **354**, 56–58.
20 N. Saifuddin, A. Z. Raziah and A. R. Junizah, *J. Chem.*, 2013, **2013**, 1–18.
21 C. Wang, K. Xia, H. Wang, X. Liang, Z. Yin and Y. Zhang, *Adv. Mater.*, 2019, **31**, 1801072.
22 L.-M. Peng, Z. Zhang and C. Qiu, *Nat. Electron.*, 2019, **2**, 499–505.
23 S. Mallakpour, E. Azadi and C. M. Hussain, *New J. Chem.*, 2021, **45**, 3756–3777.
24 C. Xiang, Y. Zhang, W. Guo and X. J. Liang, *Acta Pharm. Sin. B.*, 2020, **10**, 239–248.
25 T. Szymanski, A. A. Mieloch, M. Richter, T. Trzeciak, E. Florek, J. D. Rybka and M. Giersig, *Materials*, 2020, **13**, 4039.
26 Y. H. Teow and A. W. Mohammad, *Desalination*, 2019, **451**, 2–17.
27 X. Fan, Y. Zhou, X. Jin, R. B. Song, Z. Li and Q. Zhang, *Carbon Energy*, 2021, **3**, 449–472.
28 Y. Zhang, Q. Zhang and G. Chen, *Carbon Energy*, 2020, **2**, 408–436.
29 W. Zhao, S. Fan, N. Xiao, D. Liu, Y. Y. Tay, C. Yu, D. Sim, H. H. Hng, Q. Zhang, F. Boey, J. Ma, X. Zhao, H. Zhang and Q. Yan, *Energy Environ. Sci.*, 2012, **5**, 5364–5369.
30 A. K. K. Kyaw, H. Tantang, T. Wu, L. Ke, C. Peh, Z. H. Huang, X. T. Zeng, H. V. Demir, Q. Zhang and X. W. Sun, *Appl. Phys. Lett.*, 2011, **99**, 021107.
31 X. Zhang, W. Lu, G. Zhou and Q. Li, *Adv. Mater.*, 2020, **32**, e1902028.

32 L. Wang, S. Xie, Z. Wang, F. Liu, Y. Yang, C. Tang, X. Wu, P. Liu, Y. Li, H. Saiyin, S. Zheng, X. Sun, F. Xu, H. Yu and H. Peng, *Nat. Biomed. Eng.*, 2020, **4**, 159–171.
33 Y. Bai, H. Yue, J. Wang, B. Shen, S. Sun, S. Wang, H. Wang, X. Li, Z. Xu, R. Zhang and F. Wei, *Science*, 2020, **369**, 1104–1106.
34 R. Peng, Y. Pan, B. Liu, Z. Li, P. Pan, S. Zhang, Z. Qin, A. R. Wheeler, X. S. Tang and X. Liu, *Small*, 2021, **17**, e2100383.
35 E. Dujardin, T. W. Ebbesen, H. Hiura and K. Tanigaki, *Science*, 1994, **265**, 1850–1852.
36 T. W. Ebbesen, H. J. Lezec, H. Hiura, J. W. Bennett, H. F. Ghaemi and T. Thio, *Nature*, 1996, **382**, 54–56.
37 M. M. J. Treacy, T. W. Ebbesen and J. M. Gibson, *Nature*, 1996, **381**, 678–680.
38 J. Chen, M. A. Hamon, H. Hu, Y. S. Chen, A. M. Rao, P. C. Eklund and R. C. Haddon, *Science*, 1998, **282**, 95–98.
39 P. M. Ajayan, O. Stephan, C. Colliex and D. Trauth, *Science*, 1994, **265**, 1212–1214.
40 W. A. Deheer, W. S. Bacsa, A. Chatelain, T. Gerfin, R. Humphreybaker, L. Forro and D. Ugarte, *Science*, 1995, **268**, 845–847.
41 P. J. F. Harris, *Int. Mater. Rev.*, 2013, **49**, 31–43.
42 H. Xin and A. T. Woolley, *J. Am. Chem. Soc.*, 2003, **125**, 8710–8711.
43 C. Richard, F. Balavoine, P. Schultz, T. W. Ebbesen and C. Mioskowski, *Science*, 2003, **300**, 775–778.
44 A. Cao, V. P. Veedu, X. Li, Z. Yao, M. N. Ghasemi-Nejhad and P. M. Ajayan, *Nat. Mater.*, 2005, **4**, 540–545.
45 D. Bonifazi, C. Nacci, R. Marega, S. Campidelli, G. Ceballos, S. Modesti, M. Meneghetti and M. Prato, *Nano Lett.*, 2006, **6**, 1408–1414.
46 M. Grzelczak, M. A. Correa-Duarte and L. M. Liz-Marzán, *Small*, 2006, **2**, 1174–1177.
47 W. Wu, N. V. Tsarevsky, J. L. Hudson, J. M. Tour, K. Matyjaszewski and T. Kowalewski, *Small*, 2007, **3**, 1803–1810.
48 N. Wakamatsu, H. Takamori, T. Fujigaya and N. Nakashima, *Adv. Funct. Mater.*, 2009, **19**, 311–316.
49 M. Sanles-Sobrido, V. Salgueirino-Maceira, M. A. Correa-Duarte and L. M. Liz-Marzan, *Small*, 2008, **4**, 583–586.
50 X. Gui, J. Wei, K. Wang, A. Cao, H. Zhu, Y. Jia, Q. Shu and D. Wu, *Adv. Mater.*, 2010, **22**, 617–621.
51 Y. Shang, X. He, Y. Li, L. Zhang, Z. Li, C. Ji, E. Shi, P. Li, K. Zhu, Q. Peng, C. Wang, X. Zhang, R. Wang, J. Wei, K. Wang, H. Zhu, D. Wu and A. Cao, *Adv. Mater.*, 2012, **24**, 2896–2900.
52 M.-Q. Zhao, H.-J. Peng, G.-L. Tian, Q. Zhang, J.-Q. Huang, X.-B. Cheng, C. Tang and F. Wei, *Adv. Mater.*, 2014, **26**, 7051–7058.
53 H. Zhang, D. Wei, Y. Liu, B. Wu, L. Huang, H. Xi, J. Chen, G. Yu, H. Kajiura and Y. Li, *Small*, 2009, **5**, 2392–2396.
54 B. J. Hinds, N. Chopra, T. Rantell, R. Andrews, V. Gavalas and L. G. Bachas, *Science*, 2004, **303**, 62–65.
55 J. Wu, B. El Hamaoui, J. Li, L. Zhi, U. Kolb and K. Müllen, *Small*, 2005, **1**, 210–212.
56 J. J. Vilatela and A. H. Windle, *Adv. Mater.*, 2010, **22**, 4959–4963.
57 X. Hou, *Adv. Mater.*, 2016, **28**, 7049–7064.
58 S. Chen, Y. Tang, K. Zhan, D. Sun and X. Hou, *Nano Today*, 2018, **20**, 84–100.
59 Y. Tang, L. Cao, K. Zhan, Y. Xie, D. Sun, X. Hou and S. Chen, *Sens. Actuators, B*, 2019, **286**, 315–320.
60 M. Wang, L. Zhou, W. Deng, Y. Hou, W. He, L. Yu, H. Sun, L. Ren and X. Hou, *ACS Nano*, 2022, **16**, 2672–2681.
61 Y. Hou, M. Wang, X. Chen and X. Hou, *Nano Res.*, 2020, **14**, 8.
62 M. Wang, Y. Hou, L. Yu and X. Hou, *Nano Lett.*, 2020, **20**, 6937–6946.
63 W. He, L. Zhou, M. Wang, Y. Cao, X. Chen and X. Hou, *Sci. Bull.*, 2021, **66**, 1472–1483.
64 Y. Hou, Q. Wang, S. Wang, M. Wang, X. Chen and X. Hou, *Chin. Chem. Lett.*, 2021, DOI: 10.1016/j.cclet.2021.09.007.
65 M. Wang, H. Meng, D. Wang, Y. Yin, P. Stroeve, Y. Zhang, Z. Sheng, B. Chen, K. Zhan and X. Hou, *Adv. Mater.*, 2019, **31**, 1805130.
66 L. Yu, M. Wang and X. Hou, *Huaxue Tongbao*, 2020, **83**, 482–487.
67 R. H. Tunuguntla, R. Y. Henley, Y.-C. Yao, P. Tuan Anh, M. Wanunu and A. Noy, *Science*, 2017, **357**, 792–796.
68 J. Di, S. Li, Z. Zhao, Y. Huang, Y. Jia and H. Zheng, *Chem. Eng. J.*, 2015, **281**, 60–68.
69 C. Luo, F. Li, D. Li, Q. Fu and C. Pan, *ACS Appl. Mater. Interfaces*, 2016, **8**, 31256–31263.
70 S. Hu and Z. Xia, *Small*, 2012, **8**, 2464–2468.
71 L. Qu, L. Dai, M. Stone, Z. Xia and Z. Wang, *Science*, 2008, **322**, 238–242.
72 Y. Zhu, F. Sun, H. Qian, H. Wang, L. Mu and J. Zhu, *Chem. Eng. J.*, 2018, **338**, 670–679.
73 J. Wu, Z. Wang, W. Liu, L. Wang and F. Xu, *ACS Appl. Mater. Interfaces*, 2019, **11**, 44735–44741.
74 H. J. Lee, S. Baik, G. W. Hwang, J. H. Song, D. W. Kim, B.-Y. Park, H. Min, J. K. Kim, J.-S. Koh, T.-H. Yang and C. Pang, *ACS Nano*, 2021, **15**, 14137–14148.
75 G. Sun, C. Zhang, Z. Dai, M. Jin, Q. Liu, J. Pan, Y. Wang, X. Gao, W. Lan, G. Sun, C. Gong, Z. Zhang, X. Pan, J. Li and J. Zhou, *J. Colloid Interface Sci.*, 2022, **608**, 459–469.
76 W. Shuangquan, D. Bo, L. Ang, W. Yanfeng, Y. Qifa and Z. Lina, *Carbohydr. Polym.*, 2017, **174**, 830–840.
77 Q.-F. Guan, Z.-M. Han, K.-P. Yang, H.-B. Yang, Z.-C. Ling, C.-H. Yin and S.-H. Yu, *Nano Lett.*, 2021, **21**, 2532–2537.
78 L. Wang, Y. Wu, T. Hu, P. X. Ma and B. Guo, *Acta Biomater.*, 2019, **96**, 175–187.
79 M. Dasbach, M. Pyschik, V. Lehmann, K. Parey, D. Rhinow, H. M. Reinhardt and N. A. Hampp, *ACS Nano*, 2020, **14**, 8181–8190.
80 A. Peigney, C. Laurent, E. Flahaut, R. R. Bacsa and A. Rousset, *Carbon*, 2001, **39**, 507–514.
81 M. M. Pendergast and E. M. V. Hoek, *Energy Environ. Sci.*, 2011, **4**, 1946–1971.
82 J. Lin, X. Cai, Z. Liu, N. Liu, M. Xie, B. Zhou, H. Wang and Z. Guo, *Adv. Funct. Mater.*, 2020, **30**, 2000398.
83 Y. Yang, X. J. Li, X. Zheng, Z. Y. Chen, Q. F. Zhou and Y. Chen, *Adv. Mater.*, 2018, **30**, 1704912.

84 A. Chall, J. Stagg, A. Mixson, E. Gato, R. Quirino and V. Sittaramane, *Nanotechnology*, 2021, **32**, 195102.
85 D. Li, S. Li, J. Liu, L. Zhan, P. Wang, H. Zhu and J. Wei, *Mater. Sci. Eng., C*, 2020, **112**, 110887.
86 G. Hummer, J. C. Rasaiah and J. P. Noworyta, *Nature*, 2001, **414**, 188–190.
87 O. N. Samoylova, E. I. Calixte and K. L. Shuford, *Appl. Surf. Sci.*, 2017, **423**, 154–159.
88 R. P. Singh, G. Sharma, Sonali, S. Singh, S. Bharti, B. L. Pandey, B. Koch and M. S. Muthu, *Mater. Sci. Eng., C*, 2017, **77**, 446–458.
89 S. Xin, N. Yang, F. Gao, J. Zhao, L. Li and C. Teng, *Appl. Surf. Sci.*, 2017, **414**, 218–223.
90 H. J. Yang, J. Y. Cho, J. H. Kim, H. Y. Kim, J.-W. Lee, J. W. Wang, J. H. Kwak, S. Jung, J. H. Park, H. J. Jeong, S. Y. Jeong, S. H. Seo, G.-W. Lee and J. T. Han, *Carbon*, 2020, **157**, 649–655.
91 L. Wang, D. Zhu, J. Chen, Y. Chen and W. Chen, *Environ. Sci.: Nano*, 2017, **4**, 558–564.
92 Y. C. Jung, H. Muramatsu, K. Fujisawa, J. H. Kim, T. Hayashi, Y. A. Kim, M. Endo, M. Terrones and M. S. Dresselhaus, *Small*, 2011, **7**, 3292–3297.
93 J. Liu, C. Wang, X. Wang, X. Wang, L. Cheng, Y. Li and Z. Liu, *Adv. Funct. Mater.*, 2015, **25**, 384–392.
94 Z. Yin, X. Liang, K. Zhou, S. Li, H. Lu, M. Zhang, H. Wang, Z. Xu and Y. Zhang, *Small*, 2021, **17**, 2100066.
95 Z. Wang, J. Wu, X. Wei, S. Saleemi, W. Liu, W. Li, I. Marriam and F. Xu, *J. Mater. Chem. C*, 2020, **8**, 117–123.
96 L. Han, K. Liu, M. Wang, K. Wang, L. Fang, H. Chen, J. Zhou and X. Lu, *Adv. Funct. Mater.*, 2018, **28**, 1704195.
97 Z. Wang, S. Zhao, H. Kang, W. Zhang, S. Zhang and J. Li, *Appl. Surf. Sci.*, 2018, **434**, 1086–1100.
98 Y. Wang, S. Wu, Q. Yin, K. Du, Q. Yin, B. Jiang and S. Mo, *ACS Appl. Mater. Interfaces*, 2021, **13**, 23970–23982.
99 D. Wu, C. Yu and W. Zhong, *J. Mater. Chem. A*, 2021, **9**, 18356–18368.
100 G. Zhou, L. Mo, C. Zhou, Y. Wu, F. Lai, Y. Lv, J. Ma, Y.-E. Miao and T. Liu, *Chem. Eng. J.*, 2021, **420**, 127597.
101 P. Bhattacharya, M. Kota, D. H. Suh, K. C. Roh and H. S. Park, *Adv. Energy. Mater.*, 2017, **7**, 1700331.
102 Z.-Z. Pan, W. Lv, Y.-B. He, Y. Zhao, G. Zhou, L. Dong, S. Niu, C. Zhang, R. Lyu, C. Wang, H. Shi, W. Zhang, F. Kang, H. Nishihara and Q.-H. Yang, *Adv. Sci.*, 2018, **5**, 1800384.
103 L. Ran, B. Luo, I. R. Gentle, T. Lin, Q. Sun, M. Li, M. M. Rana, L. Wang and R. Knibbe, *ACS Nano*, 2020, **14**, 8826–8837.
104 X. Sun, M. Li, A. Ndahimana, P. Ding, Y. Xu, Q. Hu, K. Chen and T. Feng, *Energy Environ. Mater.*, 2021, **4**, 399–406.
105 W. Li, Y. Li, M. Sheng, S. Cui, Z. Wang, X. Zhang, C. Yang, Z. Yu, Y. Zhang, S. Tian, Z. Dai and Q. Xu, *Langmuir*, 2019, **35**, 4527–4533.
106 M. Peng, D. Shi, Y. Sun, J. Cheng, B. Zhao, Y. Xie, J. Zhang, W. Guo, Z. Jia, Z. Liang and L. Jiang, *Adv. Mater.*, 2020, **32**, 1908201.
107 Z. Zhang, Z. Chen, Y. Wang and Y. Zhao, *Proc. Natl. Acad. Sci. U. S. A.*, 2020, **117**, 18310–18316.
108 Y. Yang, Z. Chen, X. Song, Z. Zhang, J. Zhang, K. K. Shung, Q. Zhou and Y. Chen, *Adv. Mater.*, 2017, **29**, 1605750.
109 X. Wang, Y. He, X. Liu and J. Zhu, *Powder Technol.*, 2017, **321**, 276–285.
110 X. Yue, M. He, T. Zhang, D. Yang and F. Qu, *ACS Appl. Mater. Interfaces*, 2020, **12**, 12285–12293.
111 F. De Nicola, P. Hines, M. De Crescenzi and N. Motta, *Carbon*, 2016, **108**, 262–267.
112 J. Wu, Z. Yan, Z. Li, C. Yan, S. Lu, M. Dong and N. Yan, *Science*, 2015, **350**, aad2395.
113 J. Payandeh, T. Scheuer, N. Zheng and W. A. Catterall, *Nature*, 2011, **475**, 353–359.
114 J. Koefinger, G. Hummer and C. Dellago, *Phys. Chem. Chem. Phys.*, 2011, **13**, 15403–15417.
115 R. Garcia-Fandino and M. S. P. Sansom, *Proc. Natl. Acad. Sci. U. S. A.*, 2012, **109**, 6939–6944.
116 Y.-C. Yao, A. Taqieddin, M. A. Alibakhshi, M. Wanunu, N. R. Aluru and A. Noy, *ACS Nano*, 2019, **13**, 12851–12859.
117 J. Geng, K. Kim, J. Zhang, A. Escalada, R. Tunuguntla, L. R. Comolli, F. I. Allen, A. V. Shnyrova, K. R. Cho, D. Munoz, Y. M. Wang, C. P. Grigoropoulos, C. M. Ajo-Franklin, V. A. Frolov and A. Noy, *Nature*, 2014, **514**, 612–615.
118 K. Kim, J. Geng, R. Tunuguntla, L. R. Comolli, C. P. Grigoropoulos, C. M. Ajo-Franklin and A. Noy, *Nano Lett.*, 2014, **14**, 7051–7056.
119 R. H. Tunuguntla, F. I. Allen, K. Kim, A. Belliveau and A. Noy, *Nat. Nanotechnol.*, 2016, **11**, 639–644.
120 J. R. Sanborn, X. Chen, Y.-C. Yao, J. A. Hammons, R. H. Tunuguntla, Y. Zhang, C. C. Newcomb, J. A. Soltis, J. J. De Yoreo, A. Van Buuren, A. N. Parikh and A. Noy, *Adv. Mater.*, 2018, **30**, 1803355.
121 J. Rabinowitz, C. Cohen and K. L. Shepard, *Nano Lett.*, 2020, **20**, 1148–1153.
122 U. Narayan-Maiti, *Adv. Mater.*, 2014, **26**, 40–67.
123 J. Wu, K. Gerstandt, M. Majumder, X. Zhan and B. J. Hinds, *Nanoscale*, 2011, **3**, 3321–3328.
124 B. Hinds, *Curr. Opin. Solid State Mater. Sci.*, 2012, **16**, 1–9.
125 M. Wang, H. Meng, D. Wang, Y. Yin, P. Stroeve, Y. Zhang, Z. Sheng, B. Chen, K. Zhan and X. Hou, *Adv. Mater.*, 2019, **31**, 1805130.
126 S. Dong, Z. Gan, X. Chen, Y. Pei, B. Li, J. Ren, Y. Wang, H. He and S. Ling, *Mater. Chem. Front.*, 2021, **5**, 5706–5717.
127 M. Lu, Q. He, Y. Li, F. Guo and Z. Dai, *Carbon*, 2019, **142**, 592–598.
128 K. Zhang, W. Gong, Z. Li, W. Xu and Y. Yao, *Carbon*, 2021, **176**, 540–547.
129 V. Choudhary, B. P. Singh and R. B. Mathur, Carbon Nanotubes and Their Composites, in *Syntheses and Applications of Carbon Nanotubes and Their Composites*, 2013, pp. 193–222, DOI: 10.5772/52897.
130 F. X. Cao, P. F. Jiang, J. Z. Wang and F. Y. Yan, *Polym. Adv. Technol.*, 2018, **29**, 767–774.
131 M. S. Ata and I. Zhitomirsky, *Mater. Manuf. Processes*, 2016, **31**, 67–73.

132 Y. Sun, Y. Wang, X. Sui, W. Liang, L. He, F. Wang and B. Yang, *ACS Appl. Nano Mater.*, 2021, **4**, 10852–10863.
133 H. Min, S. Baik, J. Kim, J. Lee, B. G. Bok, J. H. Song, M. S. Kim and C. Pang, *Adv. Funct. Mater.*, 2021, 2107285.
134 M. He, H. Liu, L. Wang, X. Qin and J. Yu, *Mater. Chem. Front.*, 2021, **5**, 3673–3680.
135 X. Yin, Y. He, H. Li, X. Ma, L. Zhou, T. He and S. Li, *J. Colloid Interface Sci.*, 2021, **592**, 87–94.
136 B. Chen, G. Zhong, P. G. Oppenheimer, C. Zhang, H. Tornatzky, S. Esconjauregui, S. Hofmann and J. Robertson, *ACS Appl. Mater. Interfaces*, 2015, **7**, 3626–3632.
137 K. Ji, G. Meng, C. Yuan, E. Cui, Y. Li, J. Sun and Z. Dai, *J. Manuf. Process.*, 2018, **33**, 238–244.
138 C. F. Schaber, T. Heinlein, G. Keeley, J. J. Schneider and S. N. Gorb, *Carbon*, 2015, **94**, 396–404.
139 X. Yang, L. Chen, P. Zhang, H. Zhong, Y. Zhang, R. Zhang, P. Gu and Y. Zhao, *Nanotechnology*, 2020, **31**, 295701.
140 S. Soylemez, B. Yoon, L. Toppare and T. M. Swager, *ACS Sens.*, 2017, **2**, 1123–1127.
141 B. Zou, Y. Chu and J. Xia, *Bioprocess Biosyst. Eng.*, 2019, **42**, 279–290.
142 W. Li, Y. Gao, J. Zhang, X. Wang, F. Yin, Z. Li and M. Zhang, *Nanoscale Adv.*, 2020, **2**, 717–723.
143 S. Zhu, X.-E. Zhao, J. You, G. Xu and H. Wang, *Analyst*, 2015, **140**, 6398–6403.
144 H. Wang, P. Li, D. Yu, Y. Zhang, Z. Wang, C. Liu, H. Qiu, Z. Liu, J. Ren and X. Qu, *Nano Lett.*, 2018, **18**, 3344–3351.
145 B. Zhang, Y. He, B. Liu and D. Tang, *Anal. Chim. Acta*, 2014, **851**, 49–56.
146 D. Xu, L. Sun, Z. Zhang, Y. Wang, X. Zhang, F. Ye, Y. Zhao and J. Pan, *Appl. Mater. Today*, 2021, **24**, 101124.
147 Z. Yin, M. Jian, C. Wang, K. Xia, Z. Liu, Q. Wang, M. Zhang, H. Wang, X. Liang, X. Liang, Y. Long, X. Yu and Y. Zhang, *Nano Lett.*, 2018, **18**, 7085–7091.
148 M. Liu, X. Pu, C. Jiang, T. Liu, X. Huang, L. Chen, C. Du, J. Sun, W. Hu and Z. L. Wang, *Adv. Mater.*, 2017, **29**, 1703700.
149 M. Zhang, M. Zhao, M. Jian, C. Wang, A. Yu, Z. Yin, X. Liang, H. Wang, K. Xia, X. Liang, J. Zhai and Y. Zhang, *Matter*, 2019, **1**, 168–179.
150 H. Huang, M. Liu, D. Xu, L. Mao, Q. Huang, F. Deng, J. Tian, Y. Wen, X. Zhang and Y. Wei, *Mater. Sci. Eng., C*, 2020, **106**, 110157.
151 C. Jeong, H. Ko, H.-T. Kim, K. Sun, T.-H. Kwon, H. E. Jeong and Y.-B. Park, *ACS Appl. Mater. Interfaces*, 2020, **12**, 18813–18822.
152 S. Xia, S. Song, F. Jia and G. Gao, *J. Mater. Chem. B*, 2019, **7**, 4638–4648.
153 Y. Ben-Shimon and A. Ya'akobovitz, *Measurement*, 2021, **172**, 108889.
154 H. Wang, S. Li, Y. Wang, H. Wang, X. Shen, M. Zhang, H. Lu, M. He and Y. Zhang, *Adv. Mater.*, 2020, **32**, 1908214.